Waves in Random and Complex Media
Vol. xx, No. x, xxxxx 2006, 1–23

Taylor & Francis
Taylor & Francis

Extension of the local curvature approximation to third order and improved tilt invariance

TANOS M. ELFOUHAILY† and JOEL T. JOHNSON‡

† Rosenstiel School of Marine and Atmospheric Science, University of Miami, Florida, USA;
also at: Centre National de la Recherche Scientifique, IRPHE, Marseille, France
‡Department of Electrical and Computer Engineering, and ElectroScience Laboratory, The Ohio State University, Columbus, Ohio, USA

(Accepted February 17, 2006)

The second-order local curvature approximation (LCA2) is a theory of rough surface scattering that reproduces fundamental low and high frequency limits in a tilted frame of reference. Although the existing LCA2 model provides agreement with the first order small perturbation method up to the first order in surface tilt, results reported in this paper produce a new formulation of the model that achieves consistency with perturbation theory to first order in surface height and arbitrary order in surface tilt. In addition, extension of the modified LCA to third order is presented, and allows the theory to match the second-order small perturbation method to arbitrary order in surface tilt. Crucial to the development of the theory are a set of identities involving relationships among the small perturbation method (i.e. low frequency) and Kirchhoff approximation (i.e. high frequency) kernels; a set of new identities obtained in our derivations is also presented. Sample results involving 3D electromagnetic scattering from penetrable rough surfaces, as well as 2D scattering from Dirichlet sinusoidal gratings, are provided to compare the new results with the existing LCA2 model and with other rough surface scattering theories.

Keywords: Q1

1. Introduction

Rough surface scattering is an important branch of acoustic/electromagnetic wave physics. Any advance in this area could be beneficial for several applications ranging from medical imaging to Earth or extraterrestrial remote sensing.

The classical solutions for this problem are based either on low- or high-frequency approximations. The low-frequency approximation is known as the small perturbation method (SPM) [1, 2], and provides a perturbation series solution to the scattering problem assuming the surface height is small compared to the incident wavelength. Results from this model will be termed SPM1, SPM2, etc. in this paper depending on the order in surface height at which the perturbation series is truncated. It is well known that the SPM1 solution produces a Bragg scattering response from the surface, wherein the scattered power at a particular angle is directly proportional to the energy in a particular surface length scale. An arbitrary order

*Corresponding author. E-mail: telfouhaily@rsmas.miami.edu

Waves in Random and Complex Media
ISSN: 1745-5030 (print), 1745-5049 (online)
http://www.tandf.co.uk/journals
DOI: 10.1080/17455030600643572

SPM solution has been presented in [3]. Under a high-frequency assumption, the Kirchhoff approximation (KA) [4, 5] is obtained; this theory will be termed KA1, KA2, ... similarly in what follows, depending on the order of scattering interactions with the surface considered. Obtaining higher-order series terms in the high-frequency limit is difficult, and typically only first-order interactions are assumed.

A recent review paper [6] discusses several theories of rough surface scattering that have been developed in recent years to bridge between the classical limits. One group of recent publications [7–9] describes a new set of surface scattering models that account not only for local surface slope but also local surface curvature while satisfying most of the fundamental symmetries of the physical problem. One of these advances was termed the local curvature approximation (LCA); this model obtains compliance with KA1 as well as with the SPM1 in any rotated frame of reference up to the first order in the tilting angle of the surface. However, the model does not reproduce SPM2, KA2, or any other higher-order limits. Because the LCA expresses scattered fields as a series of terms with the KA1 solution as the first term, it can be considered as a generalization of the models by [10–12], and [13]. It also shares the same functional structure as the small slope approximation (SSA) introduced in [14–17].

Recent research into properties of the SPM and KA 'kernel' functions has revealed a set of fundamental relationships that hold; see [6] for one of the more crucial results. These identities are utilized in this paper to develop an improved LCA theory that achieves compliance with SPM1 up to arbitrary order in the tilt vector. New identities presented in this paper also allow extension of the improved LCA theory up to third order so that compliance with SPM2 is achieved to arbitrary order in surface tilt. The development of these new models is described in this paper, and sample results are provided to compare performance of the existing and new LCA theories.

The next section introduces the notation to be used throughout the paper, while section 3 defines the basic form of the LCA and reviews the basic properties it must satisfy. A discussion of the tilt invariance property follows in section 4, followed by determination of the kernels of the new model in section 5. Sample results utilizing the new model are provided in section 6.

2. Notation and definitions

2.1 *Problem definition and scattering amplitude*

For a detailed description of the scattering problem at hand the reader is referred to [6]. An electromagnetic or an acoustic wave propagating in vacuum encounters an interface (Σ) with a second half-space with a different wave propagation velocity. The scattering problem is described by the propagation directions of the incident and scattered waves in the free-space region, here labeled $\boldsymbol{K}_0$ and $\boldsymbol{K}$, respectively. These are three dimensional vectors; reference to 'horizontal' and 'vertical' parts of these vectors implies choice of a coordinate system. In order to simplify the discussion of tilt invariance, notations are adopted in this paper that attempt to make any coordinate system dependencies explicit. The vector $\boldsymbol{Q}$ is defined as $\boldsymbol{K} - \boldsymbol{K}_0$, and the wavenumber in the vacuum medium is denoted by K.

The rough boundary between the two media is described by a set of three dimensional vectors, in which each vector (labeled $\boldsymbol{R}$) extends from a specified origin to a point on the surface boundary. This set of vectors can be parametrized in terms of a pair of parameters, typically taken as the horizontal coordinates when a coordinate system is chosen. Effects on scattering predictions due to choice of the origin for the set of $\boldsymbol{R}$ vectors will be considered in section 3.2.

The scattered field above and far away from the surface is related to the incident one through the scattering operator which reads in dyadic notation (in the far field at $R \to \infty$),

$$\boldsymbol{E}_s(\boldsymbol{R}) = 2\pi \frac{\mathrm{e}^{\mathrm{i}KR}}{\mathrm{i}R} \mathbf{S}(\boldsymbol{K}, \boldsymbol{K}_0) \cdot \boldsymbol{E}_0, \tag{1}$$

which is a direct consequence of the Weyl representation of the Green's function. A similar form without the spherical wave factor is applicable for the case of scattering from a periodic surface. Here the incident plane wave field is written as

$$\boldsymbol{E}_i = \boldsymbol{E}_0 e^{i\boldsymbol{K}_0 \cdot \boldsymbol{R}} \tag{2}$$

on the surface boundary. The dyad $\mathbf{S}(\boldsymbol{K}, \boldsymbol{K}_0)$ is termed the scattering amplitude in what follows. This scattering amplitude when computed exactly is independent of the coordinate system used to describe the scattering problem.

2.2 *Polarization basis for vector problems*

When considering vector scattering problems, it is convenient to define horizontal ($\hat{\boldsymbol{H}}$) and vertical ($\hat{\boldsymbol{V}}$) polarization unit vectors. To avoid reference to a particular coordinate system, polarization vectors are defined as

$$\hat{\boldsymbol{H}}_{\boldsymbol{i}} = \hat{\boldsymbol{K}} \times \hat{\boldsymbol{K}}_{\boldsymbol{0}} / |\hat{\boldsymbol{K}} \times \hat{\boldsymbol{K}}_{\boldsymbol{0}}| \tag{3}$$

$$\hat{\boldsymbol{H}}_{\boldsymbol{s}} = \hat{\boldsymbol{H}}_{\boldsymbol{i}} \tag{4}$$

$$\hat{\boldsymbol{V}}_{\boldsymbol{i}} = \hat{\boldsymbol{H}}_{\boldsymbol{i}} \times \hat{\boldsymbol{K}}_{\boldsymbol{0}} \tag{5}$$

$$\hat{\boldsymbol{V}}_{\boldsymbol{s}} = \hat{\boldsymbol{H}}_{\boldsymbol{s}} \times \hat{\boldsymbol{K}} \tag{6}$$

where the subscripts i and s refer to the incident and scattered field, respectively. Note this polarization basis is distinct from that of most references, and involves definitions of the incident polarization basis that vary as the scattering angle of interest varies. Again this choice is adopted due to its coordinate system independence. Problems involving backscattering require independent specification of the polarization vectors, which can be chosen perpendicular to the incident direction in any manner deemed preferable.

These definitions allow the dyadic properties of $\mathbf{S}(\boldsymbol{K}, \boldsymbol{K}_0)$ to be written as

$$\mathbf{S}(\boldsymbol{K}, \boldsymbol{K}_0) = \hat{\boldsymbol{H}}_{\boldsymbol{s}} S_{HH} \hat{\boldsymbol{H}}_{\boldsymbol{i}} + \hat{\boldsymbol{V}}_{\boldsymbol{s}} S_{VH} \hat{\boldsymbol{H}}_{\boldsymbol{i}} + \hat{\boldsymbol{H}}_{\boldsymbol{s}} S_{HV} \hat{\boldsymbol{V}}_{\boldsymbol{i}} + \hat{\boldsymbol{V}}_{\boldsymbol{s}} S_{VV} \hat{\boldsymbol{V}}_{\boldsymbol{i}} \tag{7}$$

where the left unit vectors represent the scattered field polarization and the right unit vectors are dotted into the polarization of the incident field in equation (1). This polarization basis is utilized for all dyadic quantities throughout the paper.

2.3 *Coordinate system specific quantities*

In some cases (for example, in the SPM) specification of a coordinate system is unavoidable when describing the scattering amplitude. In this case, the coordinate system utilized is described by a normal vector $\hat{\boldsymbol{n}}$, which represents the 'vertical' direction in the chosen coordinate system (i.e. $\hat{\boldsymbol{n}}$ points from the surface into the vacuum region.) In this case, 'perpendicular' and 'parallel' projection operators can be defined as

$$\mathbf{P}_{\perp}(\hat{\boldsymbol{n}}) = \hat{\boldsymbol{n}}\hat{\boldsymbol{n}} \tag{8}$$

$$\mathbf{P}_{\parallel}(\hat{\boldsymbol{n}}) = \mathbf{I} - \hat{\boldsymbol{n}}\hat{\boldsymbol{n}} \tag{9}$$

where $\mathbf{I}$ is the identity dyad. These dyads produce the vector perpendicular and parallel components, respectively, when multiplying a specified vector. When choice of a coordinate system is implied in the definition of a scattering amplitude, the scattering amplitude is written as $\mathbf{S}(\boldsymbol{K}, \boldsymbol{K}_0 \mid \hat{\boldsymbol{n}})$.

Using a Cartesian system, it is possible to define a pair of orthogonal unit vectors for 'parallel' quantities. These vectors are labeled $\hat{\boldsymbol{a}}$ and $\hat{\boldsymbol{b}}$ in what follows, and are defined using an $\hat{\boldsymbol{a}} \times \hat{\boldsymbol{b}} = \hat{\boldsymbol{n}}$ convention. A specific choice for $\hat{\boldsymbol{a}}$ is avoided at present.

Given these definitions, a vector $\boldsymbol{R}$ can be written as

$$\boldsymbol{R} = \hat{\boldsymbol{a}} a + \hat{\boldsymbol{b}} b + \hat{\boldsymbol{n}} h(a, b \mid \hat{\boldsymbol{n}}) \tag{10}$$

where

$$a = \hat{\boldsymbol{a}} \cdot \boldsymbol{R} \tag{11}$$

$$b = \hat{\boldsymbol{b}} \cdot \boldsymbol{R} \tag{12}$$

$$h(a, b \mid \hat{\boldsymbol{n}}) = \hat{\boldsymbol{n}} \cdot \boldsymbol{R}. \tag{13}$$

The latter quantity represents the rough surface 'height' in the specified coordinate system, and is written as a function of the horizontal spatial coordinates. The same symbol is used to represent the corresponding surface Fourier coefficients when the arguments have the units of wavenumber:

$$h(\mathbf{P}_{\parallel}(\hat{\boldsymbol{n}}) \cdot \boldsymbol{\xi}) = \left(\frac{1}{2\pi}\right)^2 \int \mathrm{e}^{-\mathrm{i}(\mathbf{P}_{\parallel}(\hat{\boldsymbol{n}}) \cdot \boldsymbol{\xi}) \cdot (\mathbf{P}_{\parallel}(\hat{\boldsymbol{n}}) \cdot \boldsymbol{R})} h(a, b \mid \hat{\boldsymbol{n}}) \mathrm{d}(\mathbf{P}_{\parallel}(\hat{\boldsymbol{n}}) \cdot \boldsymbol{R}) \tag{14}$$

which can be written more simply as

$$h(\xi_a, \xi_b \mid \hat{\boldsymbol{n}}) = \left(\frac{1}{2\pi}\right)^2 \int \mathrm{e}^{-\mathrm{i}(\xi_a a + \xi_b b)} \, h(a, b \mid \hat{\boldsymbol{n}}) \, \mathrm{d}a \mathrm{d}b \tag{15}$$

$$h(a, b \mid \hat{\boldsymbol{n}}) = \int \mathrm{e}^{\mathrm{i}(\xi_a a + \xi_b b)} \, h(\xi_a, \xi_b \mid \hat{\boldsymbol{n}}) \, \mathrm{d}\xi_a \mathrm{d}\xi_b. \tag{16}$$

2.4 *Kirchhoff and SPM kernels for the vector dielectric case*

To help illustrate the notation utilized, scattering amplitudes from the KA and SPM theories are reviewed in this section for the case of vector scattering from a dielectric interface with relative permitivity ϵ. The KA states

$$\mathbf{S}(\boldsymbol{K}, \boldsymbol{K}_0 \mid \hat{\boldsymbol{n}}) \approx \frac{\mathcal{K}(\boldsymbol{K}, \boldsymbol{K}_0)}{Q_n} \int \mathrm{e}^{-\mathrm{i}\boldsymbol{Q} \cdot \boldsymbol{R}} \mathrm{d}(\mathbf{P}_{\parallel}(\hat{\boldsymbol{n}}) \cdot \boldsymbol{R}) \tag{17}$$

$$= \frac{\mathcal{K}(\boldsymbol{K}, \boldsymbol{K}_0)}{Q_n} \int \mathrm{e}^{-\mathrm{i}\boldsymbol{Q} \cdot \boldsymbol{R}} \mathrm{d}a \mathrm{d}b \tag{18}$$

where in the specified polarization basis,

$$\mathcal{K}(\boldsymbol{K}, \boldsymbol{K}_0) = \frac{-Q^2}{2} (\hat{\boldsymbol{H}}_s R_{HH}(Q/2) \hat{\boldsymbol{H}}_i + \hat{\boldsymbol{V}}_s R_{VV}(Q/2) \hat{\boldsymbol{V}}_i) \tag{19}$$

with

$$Q_n = \hat{\boldsymbol{n}} \cdot \boldsymbol{Q} \tag{20}$$

$$Q = |\boldsymbol{Q}| \tag{21}$$

$$R_{HH}(\beta) = \frac{\beta - \sqrt{(\epsilon-1)K^2+\beta^2}}{\beta + \sqrt{(\epsilon-1)K^2+\beta^2}} \tag{22}$$

$$R_{VV}(\beta) = \frac{\epsilon\beta - \sqrt{(\epsilon-1)K^2+\beta^2}}{\epsilon\beta + \sqrt{(\epsilon-1)K^2+\beta^2}}. \tag{23}$$

Although the KA kernel $\mathcal{K}$ is independent of any choice of coordinate system, the KA scattering amplitude (equation (17)) appears to depend on the choice of $\hat{\boldsymbol{n}}$. However, it will be shown in section 5.1 that the KA scattering amplitude in fact is independent of the coordinate system, as has been shown in [13] for the scalar problem.

The SPM expansion of the scattering amplitude states

$$\begin{aligned}\left(\frac{1}{2\pi}\right)^2 \mathbf{S}(\boldsymbol{K}, \boldsymbol{K}_0 \mid \hat{\boldsymbol{n}}) = {} & \frac{1}{Q_n}\mathbf{B}(\boldsymbol{K}, \boldsymbol{K}_0 \mid \hat{\boldsymbol{n}})\delta(Q_a)\delta(Q_b) - \mathrm{i}\mathbf{B}(\boldsymbol{K}, \boldsymbol{K}_0 \mid \hat{\boldsymbol{n}})h(Q_a, Q_b \mid \hat{\boldsymbol{n}}) \\ & - Q_n \int \mathrm{d}\xi_a \mathrm{d}\xi_b \mathbf{B}_2(\boldsymbol{K}, \boldsymbol{K}_0; \hat{\boldsymbol{a}}\xi_a + \hat{\boldsymbol{b}}\xi_b \mid \hat{\boldsymbol{n}}) h(K_a - \xi_a, K_b - \xi_b \mid \hat{\boldsymbol{n}}) \\ & \times h(\xi_a - K_{0a}, \xi_b - K_{0b} \mid \hat{\boldsymbol{n}}) + \ldots,\end{aligned} \tag{24}$$

where the subscripts a and b refer to components of the corresponding vectors along the $\hat{\boldsymbol{a}}$ and $\hat{\boldsymbol{b}}$ directions, e.g. $Q_a = \hat{\boldsymbol{a}} \cdot \boldsymbol{Q}$. Convergence of this expansion is dictated by the magnitude of $Kh(a, b|\hat{\boldsymbol{n}})$, along with the magnitude of the surface slopes in the specified coordinate system, both of which are assumed to be small.

The dyadic quantities $\mathbf{B}(\boldsymbol{K}, \boldsymbol{K}_0 \mid \hat{\boldsymbol{n}})$ and $\mathbf{B}_2(\boldsymbol{K}, \boldsymbol{K}_0; \boldsymbol{\xi} \mid \hat{\boldsymbol{n}})$ are the first- and second-order SPM 'kernels', respectively. Most references (for example [18]) utilize a coordinate system dependent polarization basis for reporting these kernels, defined as:

$$\begin{aligned}\hat{\boldsymbol{h}}_i &= \hat{\boldsymbol{K}}_{\mathbf{0}} \times \hat{\boldsymbol{n}}/|\hat{\boldsymbol{K}}_{\mathbf{0}} \times \hat{\boldsymbol{n}}| \\ \hat{\boldsymbol{h}}_s &= \hat{\boldsymbol{K}} \times \hat{\boldsymbol{n}}/|\hat{\boldsymbol{K}} \times \hat{\boldsymbol{n}}| \\ \hat{\boldsymbol{v}}_i &= \hat{\boldsymbol{h}}_i \times \hat{\boldsymbol{K}}_{\mathbf{0}} \\ \hat{\boldsymbol{v}}_s &= \hat{\boldsymbol{h}}_s \times \hat{\boldsymbol{K}}\end{aligned} \tag{25}$$

so that

$$\mathbf{S}(\boldsymbol{K}, \boldsymbol{K}_0 \mid \hat{\boldsymbol{n}}) = \hat{\boldsymbol{h}}_s S_{hh} \hat{\boldsymbol{h}}_i + \hat{\boldsymbol{v}}_s S_{vh} \hat{\boldsymbol{h}}_i + \hat{\boldsymbol{h}}_s S_{hv} \hat{\boldsymbol{v}}_i + \hat{\boldsymbol{v}}_s S_{vv} \hat{\boldsymbol{v}}_i. \tag{26}$$

However, the above dyad can be transformed easily to the $(\hat{\boldsymbol{H}}, \hat{\boldsymbol{V}})$ basis by substituting

$$\hat{\boldsymbol{h}}_i = \left(\frac{\hat{\boldsymbol{n}} \cdot \hat{\boldsymbol{V}}_i}{|\hat{\boldsymbol{n}} \times \hat{\boldsymbol{K}}_{\mathbf{0}}|}\right)\hat{\boldsymbol{H}}_i - \left(\frac{\hat{\boldsymbol{n}} \cdot \hat{\boldsymbol{H}}_i}{|\hat{\boldsymbol{n}} \times \hat{\boldsymbol{K}}_{\mathbf{0}}|}\right)\hat{\boldsymbol{V}}_i \tag{27}$$

$$\hat{\boldsymbol{h}}_s = \left(\frac{\hat{\boldsymbol{n}} \cdot \hat{\boldsymbol{V}}_s}{|\hat{\boldsymbol{n}} \times \hat{\boldsymbol{K}}|}\right)\hat{\boldsymbol{H}}_s - \left(\frac{\hat{\boldsymbol{n}} \cdot \hat{\boldsymbol{H}}_s}{|\hat{\boldsymbol{n}} \times \hat{\boldsymbol{K}}|}\right)\hat{\boldsymbol{V}}_s \tag{28}$$

$$\hat{\boldsymbol{v}}_i = \left(\frac{\hat{\boldsymbol{n}} \cdot \hat{\boldsymbol{H}}_i}{|\hat{\boldsymbol{n}} \times \hat{\boldsymbol{K}}_{\mathbf{0}}|}\right)\hat{\boldsymbol{H}}_i + \left(\frac{\hat{\boldsymbol{n}} \cdot \hat{\boldsymbol{V}}_i}{|\hat{\boldsymbol{n}} \times \hat{\boldsymbol{K}}_{\mathbf{0}}|}\right)\hat{\boldsymbol{V}}_i \tag{29}$$

$$\hat{\boldsymbol{v}}_s = \left(\frac{\hat{\boldsymbol{n}} \cdot \hat{\boldsymbol{H}}_s}{|\hat{\boldsymbol{n}} \times \hat{\boldsymbol{K}}|}\right)\hat{\boldsymbol{H}}_s + \left(\frac{\hat{\boldsymbol{n}} \cdot \hat{\boldsymbol{V}}_s}{|\hat{\boldsymbol{n}} \times \hat{\boldsymbol{K}}|}\right)\hat{\boldsymbol{V}}_s \tag{30}$$

a recombining pairs of vectors to obtain the form of equation (7).

We utilize the SPM kernels defined in [18], but scaled by constant multipliers and transformed to the $(\hat{\boldsymbol{H}}, \hat{\boldsymbol{V}})$ basis for consistency with the definition of equations (19) and (24).

Explicit expressions for the first and second order kernels are provided in Appendices A and B, respectively, for the case of vector electromagnetic scattering from an interface between free space and a penetrable medium.

3. The LCA and its basic properties

The LCA has a functional structure identical to that of the SSA, and is expressed up to third 'curvature order' as [7]:

$$\mathbf{S}(\boldsymbol{K}, \boldsymbol{K}_0 \mid \hat{\boldsymbol{n}}) \approx \mathbf{S}_0(\boldsymbol{K}, \boldsymbol{K}_0 \mid \hat{\boldsymbol{n}}) + \mathbf{S}_1(\boldsymbol{K}, \boldsymbol{K}_0 \mid \hat{\boldsymbol{n}}) + \mathbf{S}_2(\boldsymbol{K}, \boldsymbol{K}_0 \mid \hat{\boldsymbol{n}}) \tag{31}$$

where

$$\mathbf{S}_0(\boldsymbol{K}, \boldsymbol{K}_0 \mid \hat{\boldsymbol{n}}) = \frac{\mathcal{K}(\boldsymbol{K}, \boldsymbol{K}_0)}{Q_n} \int \mathrm{d}a \, \mathrm{d}b \, \mathrm{e}^{-\mathrm{i}\boldsymbol{Q}\cdot\boldsymbol{R}} \tag{32}$$

$$\mathbf{S}_1(\boldsymbol{K}, \boldsymbol{K}_0 \mid \hat{\boldsymbol{n}}) = -\mathrm{i} \int \mathrm{d}a \, \mathrm{d}b \, \mathrm{e}^{-\mathrm{i}\boldsymbol{Q}\cdot\boldsymbol{R}} \left[\int \mathrm{d}\xi_a \, \mathrm{d}\xi_b \, \mathbf{T}_1(\boldsymbol{K}, \boldsymbol{K}_0; \hat{\boldsymbol{a}}\xi_a + \hat{\boldsymbol{b}}\xi_b) h(\xi_a, \xi_b \mid \hat{\boldsymbol{n}}) \mathrm{e}^{\mathrm{i}(\xi_a a + \xi_b b)} \right] \tag{33}$$

$$\begin{aligned} \mathbf{S}_2(\boldsymbol{K}, \boldsymbol{K}_0 \mid \hat{\boldsymbol{n}}) = -\frac{Q_n}{2} \int \mathrm{d}a \, \mathrm{d}b \, \mathrm{e}^{-\mathrm{i}\boldsymbol{Q}\cdot\boldsymbol{R}} \Bigg[& \int \mathrm{d}\xi_a^{(1)} \, \mathrm{d}\xi_b^{(1)} \, h\big(\xi_a^{(1)}, \xi_b^{(1)} \mid \hat{\boldsymbol{n}}\big) \mathrm{e}^{\mathrm{i}(\xi_a^{(1)} a + \xi_b^{(1)} b)} \\ & \times \int \mathrm{d}\xi_a^{(2)} \, \mathrm{d}\xi_b^{(2)} \, h\big(\xi_a^{(2)}, \xi_b^{(2)} \mid \hat{\boldsymbol{n}}\big) \mathrm{e}^{\mathrm{i}(\xi_a^{(2)} a + \xi_b^{(2)} b)} \\ & \times \mathbf{T}_2\big(\boldsymbol{K}, \boldsymbol{K}_0; \hat{\boldsymbol{a}}\xi_a^{(1)} + \hat{\boldsymbol{b}}\xi_b^{(1)}, \hat{\boldsymbol{a}}\xi_a^{(2)} + \hat{\boldsymbol{b}}\xi_b^{(2)}\big) \Bigg]. \end{aligned} \tag{34}$$

The LCA kernels $\mathbf{T}_1(\boldsymbol{K}, \boldsymbol{K}_0; \boldsymbol{\xi})$ and $\mathbf{T}_2(\boldsymbol{K}, \boldsymbol{K}_0; \boldsymbol{\xi}^{(1)}, \boldsymbol{\xi}^{(2)})$ are sought in a coordinate-free form, so that no specification of $\hat{\boldsymbol{n}}$ is required in their definition. The arguments $\boldsymbol{\xi}$ and $\boldsymbol{\xi}^{(i)}$ of these kernels are arbitrary three-dimensional vectors in general, but are specified as particular values in the LCA integrations.

Here the extension to the third series term involving $\mathbf{T}_2$ has been added based on the Taylor–Volterra expansion implicit in the original SSA formulation. By choosing the first series term as that of KA1 (i.e. with the kernel $\mathcal{K}$) as opposed to SPM1 as in the SSA, it is possible to ensure that the correction terms in the high-frequency limit involve only the surface curvature and higher-order terms. The LCA model must respect, regardless of the boundary conditions, some fundamental properties such as reciprocity, shift invariance, and tilt invariance. Here the former two properties are considered along with other basic limits of the LCA; tilt invariance is discussed in section 4.

3.1 *Reciprocity*

The reciprocity property [19] states that

$$S_{\alpha\beta}(\boldsymbol{K}, \boldsymbol{K}_0) = S_{\beta\alpha}(-\boldsymbol{K}_0, -\boldsymbol{K})(-1)^{\mu}, \tag{35}$$

where α and β are either H or V so that scalar components of the scattering amplitude dyad are described (equation (7)). The value μ is set to zero when α and β are identical, and 1 otherwise. For the LCA, this imposes

$$T_{1,\alpha\beta}(\boldsymbol{K}, \boldsymbol{K}_0; \boldsymbol{\xi}) = T_{1,\beta\alpha}(-\boldsymbol{K}_0, -\boldsymbol{K}; \boldsymbol{\xi})(-1)^{\mu} \tag{36}$$

$$T_{2,\alpha\beta}(\boldsymbol{K}, \boldsymbol{K}_0; \boldsymbol{\xi}^{(1)}, \boldsymbol{\xi}^{(2)}) = T_{2,\beta\alpha}(-\boldsymbol{K}_0, -\boldsymbol{K}; \boldsymbol{\xi}^{(1)}, \boldsymbol{\xi}^{(2)})(-1)^{\mu} \tag{37}$$

$$\mathbf{T}_2(\boldsymbol{K}, \boldsymbol{K}_0; \boldsymbol{\xi}^{(1)}, \boldsymbol{\xi}^{(2)}) = \mathbf{T}_2(\boldsymbol{K}, \boldsymbol{K}_0; \boldsymbol{\xi}^{(2)}, \boldsymbol{\xi}^{(1)}). \tag{38}$$

The last equation states that the scattering amplitude is insensitive to the order of the integration.

3.2 *Shift invariance*

Shift invariance refers to the phase-shifting (or delay in the time domain) that results from translation of the surface boundary, or equivalently from modifications of the origin of the set of $\boldsymbol{R}$ vectors:

$$\mathbf{S}(\boldsymbol{K}, \boldsymbol{K}_0)|_{\boldsymbol{R}\to\boldsymbol{R}+\Delta\boldsymbol{R}} = e^{-\mathrm{i}\boldsymbol{Q}\cdot\Delta\boldsymbol{R}}\mathbf{S}(\boldsymbol{K}, \boldsymbol{K}_0)|_{\boldsymbol{R}} \tag{39}$$

where the left-hand side scattering amplitude is evaluated with a constant vector $\Delta\boldsymbol{R}$ added to the original set of $\boldsymbol{R}$ vectors, while the right hand side is evaluated with the original set of $\boldsymbol{R}$ vectors. Shift invariance for the LCA translates into

$$\mathbf{T}_1(\boldsymbol{K}, \boldsymbol{K}_0; \mathbf{0}) = 0 \tag{40}$$

$$\mathbf{T}_2(\boldsymbol{K}, \boldsymbol{K}_0; \boldsymbol{\xi}^{(1)}, \mathbf{0}) = \mathbf{T}_2(\boldsymbol{k}, \boldsymbol{k}_0; \mathbf{0}, \boldsymbol{\xi}^{(2)}) = 0 \tag{41}$$

which means that the kernels must vanish when any argument ($\boldsymbol{\xi}$) is set to zero. To establish these identities, the Fourier coefficient definitions of equation 15 are utilized, along with a separation of the $\Delta\boldsymbol{R}$ shift into its 'horizontal' and 'normal' components given the $\hat{\boldsymbol{n}}$ used in equations (32)–(34).

3.3 *Curvature correction*

The double and triple integrals in equations (33) and (34) are called the curvature and third-order corrections since the corresponding kernels are intended to act upon the surface elevation starting from the second derivative (or curvature) and third-order derivative terms, respectively. This is guaranteed mathematically by placing the conditions

$$\boldsymbol{\nabla}\mathbf{T}_1(\boldsymbol{K}, \boldsymbol{K}_0; \mathbf{0}) = 0 \tag{42}$$

$$\boldsymbol{\nabla}_1\mathbf{T}_2(\boldsymbol{K}, \boldsymbol{K}_0; \mathbf{0}, \boldsymbol{\xi}^{(2)}) = \boldsymbol{\nabla}_2\mathbf{T}_2(\boldsymbol{K}, \boldsymbol{K}_0; \boldsymbol{\xi}^{(1)}, \mathbf{0}) = 0 \tag{43}$$

$$\boldsymbol{\nabla}_1\boldsymbol{\nabla}_2\mathbf{T}_2(\boldsymbol{K}, \boldsymbol{K}_0; \mathbf{0}, \mathbf{0}) = 0 \tag{44}$$

on the kernels. The gradient operators are taken in three dimensional space. Note conditions (41) and (44) ensure that all second-order terms in a Taylor expansion of $\mathbf{T}_2$ vanish at the origin. These conditions set the arbitrariness due to the gauge in the Taylor–Volterra expansion [9], and leave any corrections at the curvature and higher orders. This is physically sensible since the Kirchhoff approximation captures all local slope terms under the tangent plane approximation [5] in the high-frequency limit.

3.4 *Low frequency limit of LCA3*

The existing LCA2 theory was derived to match SPM1 in the low-frequency limit; however, agreement with SPM2 was not achieved. By considering the low-frequency limit of the new LCA3 equations, a set of conditions can be written to ensure agreement with SPM2 when appropriate.

The low-frequency limit of LCA3 (equation (31)) is obtained by writing

$$e^{-i\boldsymbol{Q}\cdot\boldsymbol{R}} = e^{-i(Q_a a + Q_b b + Q_n h(a,b|\hat{\boldsymbol{n}}))} \tag{45}$$

and Taylor expanding the exponential term involving h up to second order. When the resulting expression is compared to the SPM2 (equation (24)), the conditions

$$\mathcal{K}(\boldsymbol{K}, \boldsymbol{K}_0)\delta(Q_a)\delta(Q_b) = \mathbf{B}(\boldsymbol{K}, \boldsymbol{K}_0 \mid \hat{\boldsymbol{n}})\delta(Q_a)\delta(Q_b) \tag{46}$$

$$\mathbf{T}_1(\boldsymbol{K}, \boldsymbol{K}_0; \hat{\boldsymbol{a}} Q_a + \hat{\boldsymbol{b}} Q_b) = \mathbf{B}(\boldsymbol{K}, \boldsymbol{K}_0 \mid \hat{\boldsymbol{n}}) - \mathcal{K}(\boldsymbol{K}, \boldsymbol{K}_0) \tag{47}$$

and

$$\begin{aligned}\mathbf{T}_2(\boldsymbol{K}, \boldsymbol{K}_0; \hat{\boldsymbol{a}}\xi_a + \hat{\boldsymbol{b}}\xi_b, \hat{\boldsymbol{a}}(Q_a - \xi_a) + \hat{\boldsymbol{b}}(Q_b - \xi_b)) &= \mathbf{B}_2(\boldsymbol{K}, \boldsymbol{K}_0; \hat{\boldsymbol{a}}(K_a - \xi_a) \\ &+ \hat{\boldsymbol{b}}(K_b - \xi_b) \mid \hat{\boldsymbol{n}}) + \mathbf{B}_2(\boldsymbol{K}, \boldsymbol{K}_0; \hat{\boldsymbol{a}}(K_{0a} + \xi_a) + \hat{\boldsymbol{b}}(K_{0b} + \xi_b) \mid \hat{\boldsymbol{n}}) \\ &- \mathbf{T}_1(\boldsymbol{K}, \boldsymbol{K}_0; \hat{\boldsymbol{a}}\xi_a + \hat{\boldsymbol{b}}\xi_b) - \mathbf{T}_1(\boldsymbol{K}, \boldsymbol{K}_0; \hat{\boldsymbol{a}}(Q_a - \xi_a) + \hat{\boldsymbol{b}}(Q_b - \xi_b)) - \mathcal{K}(\boldsymbol{K}, \boldsymbol{K}_0)\end{aligned} \tag{48}$$

are obtained to provide a match between the two theories. Equation (46) is obtained from zeroth order terms in surface height, and expresses the fact that both Kirchhoff and SPM1 coincide when the surface is a flat plane. Equation (47) results from first order in surface height terms, and imposes that the SPM1 limit must be reached as was used in defining the existing LCA [7]. Equation (48) is obtained from the second order in surface height terms, and provides a condition on $\mathbf{T}_2$ in order to ensure compliance with the SPM2 limit. Note the explicit dependence of the SPM kernels on the surface normal vector appears to require that the $\mathbf{T}$ kernels depend on the surface normal as well. However, a method for eliminating this dependency will be shown in section 5.

4. Tilt invariance

4.1 *Definitions*

Tilt invariance expresses the fact that the scattering amplitude should not depend on the choice of coordinate system used to describe the scattering problem and surface boundary. If formal tilt invariance is achieved, the scattering amplitude $\mathbf{S}(\boldsymbol{K}, \boldsymbol{K}_0 \mid \hat{\boldsymbol{n}})$ is independent of $\hat{\boldsymbol{n}}$ and can be written as $\mathbf{S}(\boldsymbol{K}, \boldsymbol{K}_0)$.

Tilt invariance can be investigated by beginning with the scattering amplitude written in a first coordinate system $\mathbf{S}(\boldsymbol{K}, \boldsymbol{K}_0 \mid \hat{\boldsymbol{n}}_1)$. Mathematical manipulations are then performed upon the scattering amplitude expressions to attempt to make them appear as if they were written in a second coordinate system $\hat{\boldsymbol{n}}_2$. This transformed version of $\mathbf{S}(\boldsymbol{K}, \boldsymbol{K}_0 \mid \hat{\boldsymbol{n}}_1)$ is then compared to the scattering amplitude written directly in the second coordinate system $\mathbf{S}(\boldsymbol{K}, \boldsymbol{K}_0 \mid \hat{\boldsymbol{n}}_2)$. Should the two be identical, formal tilt invariance has been established. However, if the two are not identical, an expansion of the transformed $\mathbf{S}(\boldsymbol{K}, \boldsymbol{K}_0 \mid \hat{\boldsymbol{n}}_1)$ in terms of surface 'height' in the second coordinate system can be performed, and compared to the same expansion of $\mathbf{S}(\boldsymbol{K}, \boldsymbol{K}_0 \mid \hat{\boldsymbol{n}}_2)$. The level of agreement observed in the two expansions establishes the order to which the model examined reproduces a 'tilted' SPM theory.

Note this examination of tilt invariance will involve use of a formal rotation process, in contrast to the typical first order in slope tilting process that is commonly used in the literature (see for example [17].) Use of a formal tilting process is required if SPM expansions beyond first order are to be examined.

4.2 *Coordinate systems for examining tilt invariance*

The presentation to follow will involve a first coordinate system $(\hat{\boldsymbol{a}}_1, \hat{\boldsymbol{b}}_1, \hat{\boldsymbol{n}}_1)$ and a second coordinate system $(\hat{\boldsymbol{a}}_2, \hat{\boldsymbol{b}}_2, \hat{\boldsymbol{n}}_2)$, in which the normal vectors are the primary factors that determine the coordinate systems. Although the horizontal coordinates in these systems are not uniquely specified, here we adopt the definitions:

$$\hat{\boldsymbol{b}}_1 = \hat{\boldsymbol{b}}_2 = \frac{\hat{\boldsymbol{n}}_1 \times \hat{\boldsymbol{n}}_2}{|\hat{\boldsymbol{n}}_1 \times \hat{\boldsymbol{n}}_2|} \tag{49}$$

$$\hat{\boldsymbol{a}}_1 = \hat{\boldsymbol{b}}_1 \times \hat{\boldsymbol{n}}_1 \tag{50}$$

$$\hat{\boldsymbol{a}}_2 = \hat{\boldsymbol{b}}_2 \times \hat{\boldsymbol{n}}_2. \tag{51}$$

The $\hat{\boldsymbol{a}}$ and $\hat{\boldsymbol{n}}$ vectors for both frames have only $\hat{\boldsymbol{a}}$ and $\hat{\boldsymbol{n}}$ components in either coordinate system as a result of these definitions. Defining

$$\cos\alpha = \hat{\boldsymbol{n}}_1 \cdot \hat{\boldsymbol{n}}_2 \tag{52}$$

$$\sin\alpha = |\hat{\boldsymbol{n}}_1 \times \hat{\boldsymbol{n}}_2| \tag{53}$$

allows the coordinate vectors to be related as:

$$\hat{\boldsymbol{a}}_1 = \hat{\boldsymbol{a}}_2 \cos\alpha + \hat{\boldsymbol{n}}_2 \sin\alpha \tag{54}$$

$$\hat{\boldsymbol{a}}_2 = \hat{\boldsymbol{a}}_1 \cos\alpha - \hat{\boldsymbol{n}}_1 \sin\alpha \tag{55}$$

$$\hat{\boldsymbol{n}}_1 = -\hat{\boldsymbol{a}}_2 \sin\alpha + \hat{\boldsymbol{n}}_2 \cos\alpha \tag{56}$$

$$\hat{\boldsymbol{n}}_2 = \hat{\boldsymbol{a}}_1 \sin\alpha + \hat{\boldsymbol{n}}_1 \cos\alpha. \tag{57}$$

Similarly the space coordinates

$$a_1 = \hat{\boldsymbol{a}}_1 \cdot \boldsymbol{R} \tag{58}$$

$$b_1 = \hat{\boldsymbol{b}}_1 \cdot \boldsymbol{R} \tag{59}$$

$$h(a_1, b_1 \mid \hat{\boldsymbol{n}}_1) = \hat{\boldsymbol{n}}_1 \cdot \boldsymbol{R} \tag{60}$$

can be related to those in the second frame through

$$a_1 = a_2 \cos\alpha + h(a_2, b_2 \mid \hat{\boldsymbol{n}}_2) \sin\alpha \tag{61}$$

$$a_2 = a_1 \cos\alpha - h(a_1, b_1 \mid \hat{\boldsymbol{n}}_1) \sin\alpha \tag{62}$$

$$b_1 = b_2 \tag{63}$$

$$h(a_1, b_1 \mid \hat{\boldsymbol{n}}_1) = h(a_2, b_2 \mid \hat{\boldsymbol{n}}_2) \cos\alpha - a_2 \sin\alpha \tag{64}$$

$$h(a_2, b_2 \mid \hat{\boldsymbol{n}}_2) = h(a_1, b_1 \mid \hat{\boldsymbol{n}}_1) \cos\alpha + a_1 \sin\alpha. \tag{65}$$

Differential horizontal areas can be related through a Jacobian transformation to obtain

$$\mathrm{d}a_1\, \mathrm{d}b_1 = \mathrm{d}a_2\, \mathrm{d}b_2\, \cos\alpha \left(1 + \tan\alpha \frac{\partial h(a_2, b_2 \mid \hat{\boldsymbol{n}}_2)}{\partial a_2}\right). \tag{66}$$

4.3 *Transformation of surface Fourier coefficients*

Because Fourier coefficients are included in the LCA3 theory, transformation of these coefficients must also be considered in studies of tilt invariance. From equation (15), surface Fourier

coefficients in coordinate system one are

$$h(\xi_{a1}, \xi_{b1} \mid \hat{\boldsymbol{n}}_1) = \left(\frac{1}{2\pi}\right)^2 \int \mathrm{e}^{-\mathrm{i}(\xi_{a1}a_1 + \xi_{b1}b_1)}\, h(a_1, b_1 \mid \hat{\boldsymbol{n}}_1)\, \mathrm{d}a_1 \mathrm{d}b_1. \tag{67}$$

Using the Jacobian and coordinate system relationships derived in the previous section, equation (68) can be rewritten as

$$h(\xi_{a1}, \xi_{b1} \mid \hat{\boldsymbol{n}}_1) = \left(\frac{1}{2\pi}\right)^2 \cos\alpha \int \mathrm{d}a_2 \mathrm{d}b_2 \left(1 + \tan\alpha \frac{\partial h(a_2, b_2 \mid \hat{\boldsymbol{n}}_2)}{\partial a_2}\right) \times [h(a_2, b_2 \mid \hat{\boldsymbol{n}}_2)\cos\alpha - a_2 \sin\alpha] \mathrm{e}^{-\mathrm{i}((\xi_{a1}\cos\alpha)a_2) + \xi_{b1}b_2)} \mathrm{e}^{-\mathrm{i}(\xi_{a1}\sin\alpha)h(a_2, b_2 \mid \hat{\boldsymbol{n}}_2)} \tag{68}$$

Relating this expression to the surface Fourier coefficients in the second coordinate system requires expansion of the exponential function involving h into a power series. Integration by parts can be used on the resulting series; the identity

$$\frac{\partial}{\partial a_2}\left[a_2 h_2^n\right] = h_2^n + n h_2^{n-1} a_2 \frac{\partial h_2}{\partial a_2} \tag{69}$$

(where h_2 is used to notate $h(a_2, b_2 \mid \hat{\boldsymbol{n}}_2)$) is useful in this process. The final result is

$$h\left(\frac{\xi_{a1}}{\cos\alpha}, \xi_{b1} \mid \hat{\boldsymbol{n}}_1\right) = -i\delta'(\xi_{a1})\delta(\xi_{b1})\cos\alpha \sin\alpha + h(\xi_{a1}, \xi_{b1} \mid \hat{\boldsymbol{n}}_2) + \sum_{n=2}^{\infty} \frac{(-i\xi_{a1}\tan\alpha)^{n-1}}{n!} \left(\frac{1}{2\pi}\right)^2 \int \mathrm{e}^{-\mathrm{i}(\xi_{a1}a_2 + \xi_{b1}b_2)}\, h^n(a_2, b_2 \mid \hat{\boldsymbol{n}}_2)\, \mathrm{d}a_2 \mathrm{d}b_2. \tag{70}$$

The zeroth-order term contains a Dirac delta function and its derivative, while the first-order term is exactly the Fourier coefficient in the second frame. However, an infinite series of higher-order terms is also added, expressed in terms of Fourier transforms of the nth power of the surface height in the second frame. It is possible to sum the series expression to obtain a form involving a Fourier-like integration of $e^{-i\xi_{a1}\tan\alpha h(a_2, b_2 \mid \hat{\boldsymbol{n}}_2)}$; however, such a summation yields no advantages in the following analyses.

5. Tilt invariance and determination of LCA3 kernels

5.1 *Tilt invariance of Kirchhoff Approximation*

To examine tilt invariance of the LCA3 theory, begin with the $\mathbf{S}_0$ term written in coordinate system one:

$$\mathbf{S}_0(\boldsymbol{K}, \boldsymbol{K}_0 \mid \hat{\boldsymbol{n}}_1) = \frac{\mathcal{K}(\boldsymbol{K}, \boldsymbol{K}_0)}{Q_{n1}} \int \mathrm{d}a_1\, \mathrm{d}b_1\, \mathrm{e}^{-\mathrm{i}\boldsymbol{Q}\cdot\boldsymbol{R}} \tag{71}$$

$$= \frac{\mathcal{K}(\boldsymbol{K}, \boldsymbol{K}_0)\cos\alpha}{Q_{n1}} \int \mathrm{d}a_2\, \mathrm{d}b_2 \left(1 + \tan\alpha \frac{\partial h(a_2, b_2 \mid \hat{\boldsymbol{n}}_2)}{\partial a_2}\right) \mathrm{e}^{-\mathrm{i}\boldsymbol{Q}\cdot\boldsymbol{R}}$$

$$= \frac{\mathcal{K}(\boldsymbol{K}, \boldsymbol{K}_0)}{Q_{n1}} \int \mathrm{d}a_2\, \mathrm{d}b_2 \left(\cos\alpha - \sin\alpha \frac{Q_{a2}}{Q_{n2}}\right) \mathrm{e}^{-\mathrm{i}\boldsymbol{Q}\cdot\boldsymbol{R}} \tag{72}$$

with the final equation obtained through an integration by parts. Because

$$Q_{n1} = -Q_{a2}\sin\alpha + Q_{n2}\cos\alpha \tag{73}$$

we find

$$\mathbf{S}_0(\boldsymbol{K}, \boldsymbol{K}_0 \mid \hat{\boldsymbol{n}}_1) = \frac{\mathcal{K}(\boldsymbol{K}, \boldsymbol{K}_0)}{Q_{n2}} \int \mathrm{d}a_2\, \mathrm{d}b_2\, \mathrm{e}^{-\mathrm{i}\boldsymbol{Q}\cdot\boldsymbol{R}} \tag{74}$$

$$= \mathbf{S}_0(\boldsymbol{K}, \boldsymbol{K}_0 \mid \hat{\boldsymbol{n}}_2) \tag{75}$$

and the $\mathbf{S}_0$ term (the Kirchhoff Approximation) has been shown to be formally tilt invariant.

5.2 *Tilt invariance of LCA2 at first order in surface height*

Begin with $\mathbf{S}_1$ written in the first coordinate system:

$$\mathbf{S}_1(\boldsymbol{K}, \boldsymbol{K}_0 \mid \hat{\boldsymbol{n}}_1) = -\mathrm{i} \int \mathrm{d}a_1\, \mathrm{d}b_1 \int \mathrm{d}\xi_{a1}\, \mathrm{d}\xi_{b1} \mathrm{e}^{-\mathrm{i}\boldsymbol{Q}\cdot\boldsymbol{R}} \big[\mathbf{T}_1(\boldsymbol{K}, \boldsymbol{K}_0; \hat{\boldsymbol{a}}_1\xi_{a1} + \hat{\boldsymbol{b}}_1\xi_{b1}) h \times (\xi_{a1}, \xi_{b1} \mid \hat{\boldsymbol{n}}_1) \mathrm{e}^{\mathrm{i}(\xi_{a1}a_1 + \xi_{b1}b_1)}\big]. \tag{76}$$

Following a process similar to that utilized in transforming the surface Fourier coefficients, we can transform the above to

$$\mathbf{S}_1(\boldsymbol{K}, \boldsymbol{K}_0 \mid \hat{\boldsymbol{n}}_1) = -\mathrm{i} \int \mathrm{d}a_2\, \mathrm{d}b_2 \int \mathrm{d}\xi_{a1}\, \mathrm{d}\xi_{b1}\ \mathrm{e}^{-\mathrm{i}\boldsymbol{Q}\cdot\boldsymbol{R}} \frac{Q_{n1}}{Q_{n2} - \xi_{a1}\sin\alpha} \times \big[\mathbf{T}_1(\boldsymbol{K}, \boldsymbol{K}_0; \hat{\boldsymbol{a}}_1\xi_{a1} + \hat{\boldsymbol{b}}_1\xi_{b1}) h(\xi_{a1}, \xi_{b1} \mid \hat{\boldsymbol{n}}_1) \mathrm{e}^{\mathrm{i}(\xi_{a1}\cos\alpha a_2 + \xi_{b1}b_2)}\big] \times \mathrm{e}^{\mathrm{i}(\xi_{a1}\sin\alpha) h(a_2, b_2 \mid \hat{\boldsymbol{n}}_2)}. \tag{77}$$

It is convenient here to introduce a new set of variables

$$\xi_{a2} = \xi_{a1}\cos\alpha \tag{78}$$

$$\xi_{b2} = \xi_{b1} \tag{79}$$

with Jacobian

$$\mathrm{d}\xi_{a1}\, \mathrm{d}\xi_{b1} = \mathrm{d}\xi_{a2}\, \mathrm{d}\xi_{b2}\ \sec\alpha \tag{80}$$

to obtain

$$\mathbf{S}_1(\boldsymbol{K}, \boldsymbol{K}_0 \mid \hat{\boldsymbol{n}}_1) = -\mathrm{i} \int \mathrm{d}a_2\, \mathrm{d}b_2 \int \mathrm{d}\xi_{a2}\, \mathrm{d}\xi_{b2}\ \mathrm{e}^{-\mathrm{i}\boldsymbol{Q}\cdot\boldsymbol{R}} \frac{Q_{n1}}{Q_{n2}\cos\alpha - \xi_{a2}\sin\alpha} \times \left[\mathbf{T}_1(\boldsymbol{K}, \boldsymbol{K}_0; \hat{\boldsymbol{a}}_1\xi_{a2}\sec\alpha + \hat{\boldsymbol{b}}_1\xi_{b2}) h\left(\frac{\xi_{a2}}{\cos\alpha}, \xi_{b2} \mid \hat{\boldsymbol{n}}_1\right) \mathrm{e}^{\mathrm{i}(\xi_{a2}a_2 + \xi_{b2}b_2)}\right] \times \mathrm{e}^{\mathrm{i}(\xi_{a2}\tan\alpha) h(a_2, b_2 \mid \hat{\boldsymbol{n}}_2)}. \tag{81}$$

Given the additional phase factor involving h_2 introduced by the transformation, as well as the higher order terms included in the Fourier coefficients in equation (70), formal tilt invariance is not achieved by the LCA2 model. However, we can examine tilt invariance of the transformed $\mathbf{S}_1$ when expanded in surface height in the second coordinate system.

Begin by considering the expansion up to first order in h_2. First note that the Fourier coefficients $h(\frac{\xi_{a2}}{\cos\alpha}, \xi_{b2} \mid \hat{\boldsymbol{n}}_1)$ in the integration contain a term at zeroth order. However, this zeroth-order term involves a Dirac delta function and its derivative evaluated at the origin of the (ξ_{a2}, ξ_{b2}) plane. The result is that the zeroth-order Fourier coefficient term always

multiplies either $\mathbf{T}_1$ evaluated at the origin or the derivative of $\mathbf{T}_1$ at the origin. Both of these quantities will be set to zero according to equations (40) and (42), so that the zeroth-order Fourier coefficients make no contribution to the scattering amplitude.

The first-order contributions are then completely obtained from the first-order Fourier coefficient, utilizing zeroth order in h_2 forms for the remaining terms in the LCA2 integration:

$$\mathbf{S}_1(\boldsymbol{K}, \boldsymbol{K}_0 \mid \hat{\boldsymbol{n}}_1) \approx -\mathrm{i} \int \mathrm{d}a_2 \, \mathrm{d}b_2 \int \mathrm{d}\xi_{a2} \mathrm{d}\xi_{b2} \;\; \mathrm{e}^{-\mathrm{i}(Q_{a2}-\xi_{a2})a_2} \mathrm{e}^{-\mathrm{i}(Q_{b2}-\xi_{b2})b_2} \frac{Q_{n1}}{Q_{n2}\cos\alpha - \xi_{a2}\sin\alpha} \times \left[\mathbf{T}_1(\boldsymbol{K}, \boldsymbol{K}_0; \hat{\boldsymbol{a}}_1 \xi_{a2} \sec\alpha + \hat{\boldsymbol{b}}_1 \xi_{b2}) h(\xi_{a2}, \xi_{b2} \mid \hat{\boldsymbol{n}}_2) \mathrm{e}^{\mathrm{i}(\xi_{a2}a_2 + \xi_{b2}b_2)}\right]. \tag{82}$$

The integration over space yields Dirac delta functions, and the final first-order result is:

$$\mathbf{S}_1(\boldsymbol{K}, \boldsymbol{K}_0 \mid \hat{\boldsymbol{n}}_1) \approx -\mathrm{i}(2\pi)^2 \, h(Q_{a2}, Q_{b2} \mid \hat{\boldsymbol{n}}_2) \mathbf{T}_1(\boldsymbol{K}, \boldsymbol{K}_0; \hat{\boldsymbol{a}}_1 Q_{a2} \sec\alpha + \hat{\boldsymbol{b}}_1 Q_{b2}). \tag{83}$$

In order to achieve tilt invariance to first order in surface height, we must require

$$\mathbf{T}_1(\boldsymbol{K}, \boldsymbol{K}_0; \hat{\boldsymbol{a}}_1 Q_{a2} \sec\alpha + \hat{\boldsymbol{b}}_1 Q_{b2}) = \mathbf{T}_1(\boldsymbol{K}, \boldsymbol{K}_0; \hat{\boldsymbol{a}}_2 Q_{a2} + \hat{\boldsymbol{b}}_2 Q_{b2}) \tag{84}$$

$$= \mathbf{B}(\boldsymbol{K}, \boldsymbol{K}_0 \mid \hat{\boldsymbol{n}}_2) - \mathcal{K}(\boldsymbol{K}, \boldsymbol{K}_0) \tag{85}$$

Note that the argument of $\mathbf{T}_1$ on the left-hand side above can also be written as

$$\hat{\boldsymbol{a}}_1 Q_{a2} \sec\alpha + \hat{\boldsymbol{b}}_1 Q_{b2} = \boldsymbol{Q} - \hat{\boldsymbol{n}}_2 Q_{n1} \sec\alpha \tag{86}$$

In addition to these properties we also require

$$\mathbf{T}_1(\boldsymbol{K}, \boldsymbol{K}_0; 0) = 0 \tag{87}$$

and

$$\nabla \mathbf{T}_1(\boldsymbol{K}, \boldsymbol{K}_0; 0) = 0. \tag{88}$$

The identity

$$\mathbf{B}(\boldsymbol{K}, \boldsymbol{K}_0 \mid \hat{\boldsymbol{n}} = \hat{\boldsymbol{Q}}) = \mathcal{K}(\boldsymbol{K}, \boldsymbol{K}_0) \tag{89}$$

has been derived recently [6]. This identity is based on combination of the tilt invariance properties of the $\mathcal{K}$ kernel along with the well known fact that the SPM and Kirchhoff kernels yield identical predictions for specular scattering. It can also be shown that

$$\nabla \mathbf{B}\left(\boldsymbol{K}, \boldsymbol{K}_0 \mid \hat{\boldsymbol{n}} = \frac{\boldsymbol{Q} - \boldsymbol{\xi}}{|\boldsymbol{Q} - \boldsymbol{\xi}|}\right)|_{\xi=0} = 0 \tag{90}$$

which indicates that the SPM kernel varies quadratically about the specular point. These identities hold regardless of the boundary condition considered.

Combining these properties allows a $\mathbf{T}_1$ kernel with the needed properties to be found as:

$$\mathbf{T}_1(\boldsymbol{K}, \boldsymbol{K}_0; \boldsymbol{\xi}) = \mathbf{B}\left(\boldsymbol{K}, \boldsymbol{K}_0 \mid \hat{\boldsymbol{n}} = \frac{\boldsymbol{Q} - \boldsymbol{\xi}}{|\boldsymbol{Q} - \boldsymbol{\xi}|}\right) - \mathcal{K}(\boldsymbol{K}, \boldsymbol{K}_0). \tag{91}$$

This kernel is independent of the coordinate system, and produces an LCA2 theory that is tilt invariant to first order in surface height, regardless of the angle α (i.e. slope of any tilting) involved in the tilting process.

5.3 *Examination of tilt invariance of LCA3 at second order in surface height*

At second order in surface height, the $\mathbf{S}_0$ term produces contributions of

$$(-\mathrm{i})^2(2\pi)^2\left(\frac{Q_{n2}}{2}\right)\mathcal{K}(\boldsymbol{K},\boldsymbol{K}_0)$$
$$\int \mathrm{d}\xi_a\,\mathrm{d}\xi_b\; h(\xi_a,\xi_b\mid\hat{\boldsymbol{n}}_2)h(Q_{a2}-\xi_a,\,Q_{b2}-\xi_b\mid\hat{\boldsymbol{n}}_2) \tag{92}$$

while the $\mathbf{S}_1$ term produces contributions of

$$(-\mathrm{i})^2(2\pi)^2\Bigg[\left(\frac{Q_{a2}\tan\alpha}{2}\right)\mathbf{T}_1(\boldsymbol{K},\boldsymbol{K}_0;\hat{\boldsymbol{a}}_2Q_{a2}+\hat{\boldsymbol{b}}_2Q_{b2})\int \mathrm{d}\xi_a\,\mathrm{d}\xi_b\; h(\xi_a,\xi_b\mid\hat{\boldsymbol{n}}_2)$$
$$\times h(Q_{a2}-\xi_a,\,Q_{b2}-\xi_b|\hat{\boldsymbol{n}}_2)+\left(\frac{Q_{n1}\sec\alpha}{2}\right)\int \mathrm{d}\xi_a\,\mathrm{d}\xi_b\; h(\xi_a,\xi_b|\hat{\boldsymbol{n}}_2)h(Q_{a2}-\xi_a,\,Q_{b2}-\xi_b\mid\hat{\boldsymbol{n}}_2)$$
$$\times\left(\mathbf{T}_1(\boldsymbol{K},\boldsymbol{K}_0;\hat{\boldsymbol{a}}_1(Q_{a2}-\xi_a)\sec\alpha+\hat{\boldsymbol{b}}_1(Q_{b2}-\xi_b))+\mathbf{T}_1(\boldsymbol{K},\boldsymbol{K}_0;\hat{\boldsymbol{a}}_1\xi_a\sec\alpha+\hat{\boldsymbol{b}}_1\xi_b)\right)\Bigg]. \tag{93}$$

The first term above arises from the second order in height contribution of the transformed surface Fourier coefficients (equation (70)), while the second term arises from the first order in height Fourier coefficients multiplied with other first order in height terms in equation (81). A symmetrization was performed to generate the particular second term shown. The two terms are similar, although the first does not include the $\mathbf{T}_1$ kernel inside the integration, while the second does.

Following a similar process to that utilized in the previous section, a transformed version of $\mathbf{S}_2(\boldsymbol{K},\boldsymbol{K}_0|\hat{\boldsymbol{n}}_1)$ can be derived, and its second order in height h_2 terms determined. The result is

$$(-\mathrm{i})^2(2\pi)^2\frac{Q_{n1}\sec\alpha}{2}\int \mathrm{d}\xi_a\,\mathrm{d}\xi_b\; h(\xi_a,\xi_b\mid\hat{\boldsymbol{n}}_2)h(Q_{a2}-\xi_a,\,Q_{b2}-\xi_b\mid\hat{\boldsymbol{n}}_2)$$
$$\mathbf{T}_2(\boldsymbol{K},\boldsymbol{K}_0;\hat{\boldsymbol{a}}_1\xi_a\sec\alpha+\hat{\boldsymbol{b}}_1\xi_b,\hat{\boldsymbol{a}}_1(Q_{a2}-\xi_a)\sec\alpha+\hat{\boldsymbol{b}}_1(Q_{b2}-\xi_b)). \tag{94}$$

Compliance with SPM2 in the $\hat{\boldsymbol{n}}_2$ frame requires

$$\begin{aligned}
&Q_{n2}\mathbf{B}_2(\boldsymbol{K},\boldsymbol{K}_0;\hat{\boldsymbol{a}}_2(K_{a2}-\xi_a)+\hat{\boldsymbol{b}}_2(K_{b2}-\xi_b)\mid\hat{\boldsymbol{n}}_2)+Q_{n2}\mathbf{B}_2(\boldsymbol{K},\boldsymbol{K}_0;\hat{\boldsymbol{a}}_2(K_{0a2}+\xi_a)\\
&\quad+\hat{\boldsymbol{b}}_2(K_{0b2}+\xi_b)\mid\hat{\boldsymbol{n}}_2)=Q_{n2}\mathcal{K}(\boldsymbol{K},\boldsymbol{K}_0)+Q_{a2}\tan\alpha\mathbf{T}_1(\boldsymbol{K},\boldsymbol{K}_0;\hat{\boldsymbol{a}}_2Q_{a2}+\hat{\boldsymbol{b}}_2Q_{b2})\\
&\quad+Q_{n1}\sec\alpha\mathbf{T}_1(\boldsymbol{K},\boldsymbol{K}_0;\hat{\boldsymbol{a}}_1\xi_a\sec\alpha+\hat{\boldsymbol{b}}_1\xi_b)+Q_{n1}\sec\alpha\mathbf{T}_1(\boldsymbol{K},\boldsymbol{K}_0;\hat{\boldsymbol{a}}_1(Q_{a2}-\xi_a)\sec\alpha\\
&\quad+\hat{\boldsymbol{b}}_1(Q_{b2}-xi_b))+Q_{n1}\sec\alpha\mathbf{T}_2(\boldsymbol{K},\boldsymbol{K}_0;\hat{\boldsymbol{a}}_1\xi_a\sec\alpha+\hat{\boldsymbol{b}}_1\xi_b,\hat{\boldsymbol{a}}_1(Q_{a2}-\xi_a)\sec\alpha\\
&\quad+\hat{\boldsymbol{b}}_1(Q_{b2}-\xi_b)).
\end{aligned} \tag{95}$$

We also require $\mathbf{T}_2$ to vanish when either of the 3D $\boldsymbol{\xi}$ arguments is set to zero, as well as the absence of any first or second derivatives in $\boldsymbol{\xi}$ at the origin. Clearly, relationships among the $\mathbf{B}$, $\mathbf{B}_2$, and $\mathcal{K}$ kernels will be required to find an appropriate $\mathbf{T}_2$ kernel.

One such relationship is obtained by application of the shift-invariance property to the SPM expansion, which yields

$$\mathbf{B}_2(\boldsymbol{K},\boldsymbol{K}_0;\boldsymbol{K}\mid\hat{\boldsymbol{n}})+\mathbf{B}_2(\boldsymbol{K},\boldsymbol{K}_0;\boldsymbol{K}_0\mid\hat{\boldsymbol{n}})=\mathbf{B}(\boldsymbol{K},\boldsymbol{K}_0\mid\hat{\boldsymbol{n}}). \tag{96}$$

This identity was derived in [16, 20]. By combining this identity with equation (89) it is possible to obtain

$$2\mathbf{B}_2(\boldsymbol{K},\boldsymbol{K}_0;\boldsymbol{K}\mid\hat{\boldsymbol{n}}=\hat{\boldsymbol{Q}})=\mathbf{B}(\boldsymbol{K},\boldsymbol{K}_0\mid\hat{\boldsymbol{n}}=\hat{\boldsymbol{Q}})=\mathcal{K}(\boldsymbol{K},\boldsymbol{K}_0). \tag{97}$$

The third argument of $\mathbf{B}_2$ above ($\boldsymbol{K}$) can also be replaced by $\boldsymbol{K}_0$ due to the specular scattering geometry that results with $\hat{\boldsymbol{n}} = \hat{\boldsymbol{Q}}$. Comparing with equation (90) we can also find

$$\nabla \mathbf{B}_2\left(\boldsymbol{K}, \boldsymbol{K}_0; \boldsymbol{K} \pm \boldsymbol{\xi} \mid \hat{\boldsymbol{n}} = \frac{\boldsymbol{Q} - \boldsymbol{\xi}}{|\boldsymbol{Q} - \boldsymbol{\xi}|}\right)\Big|_{\xi=0} = 0. \tag{98}$$

Finally, note that if the normal vector is defined as

$$\hat{\boldsymbol{n}}' = \frac{\boldsymbol{Q} - \boldsymbol{\xi}^{(1)} - \boldsymbol{\xi}^{(2)}}{|\boldsymbol{Q} - \boldsymbol{\xi}^{(1)} - \boldsymbol{\xi}^{(2)}|} \tag{99}$$

then

$$\mathbf{P}_{\parallel}(\hat{\boldsymbol{n}}') \cdot \left(\boldsymbol{K} - \boldsymbol{\xi}^{(1)}\right) = \mathbf{P}_{\parallel}(\hat{\boldsymbol{n}}') \cdot \left(\boldsymbol{K}_0 + \boldsymbol{\xi}^{(2)}\right) \tag{100}$$

for arbitrary $\boldsymbol{\xi}^{(1)}$ and $\boldsymbol{\xi}^{(2)}$. This relationship allows arguments $\boldsymbol{K} - \boldsymbol{\xi}^{(1)}$ to be replaced with $\boldsymbol{K}_0 + \boldsymbol{\xi}^{(2)}$ when the normal vector (99) is adopted. All of identities (96)–(100) hold regardless of the surface boundary conditions (i.e. Dirichlet, Neumann, penetrable, etc.).

Combining this information allows a $\mathbf{T}_2$ kernel to be derived as

$$\begin{aligned}\mathbf{T}_2\left(\boldsymbol{K}, \boldsymbol{K}_0; \boldsymbol{\xi}^{(1)}, \boldsymbol{\xi}^{(2)}\right) = \left[\frac{\hat{\boldsymbol{n}}' \cdot \boldsymbol{Q}}{\hat{\boldsymbol{n}}' \cdot (\boldsymbol{Q} - \boldsymbol{\xi}^{(1)} - \boldsymbol{\xi}^{(2)})}\right]\Bigg\{&\mathbf{B}_2\left(\boldsymbol{K}, \boldsymbol{K}_0; \boldsymbol{K} - \boldsymbol{\xi}^{(1)} \mid \hat{\boldsymbol{n}} = \frac{\boldsymbol{Q} - \boldsymbol{\xi}^{(1)} - \boldsymbol{\xi}^{(2)}}{|\boldsymbol{Q} - \boldsymbol{\xi}^{(1)} - \boldsymbol{\xi}^{(2)}|}\right)\\ &+ \mathbf{B}_2\left(\boldsymbol{K}, \boldsymbol{K}_0; \boldsymbol{K} - \boldsymbol{\xi}^{(2)} \mid \hat{\boldsymbol{n}} = \frac{\boldsymbol{Q} - \boldsymbol{\xi}^{(1)} - \boldsymbol{\xi}^{(2)}}{\left|\boldsymbol{Q} - \boldsymbol{\xi}^{(1)} - \boldsymbol{\xi}^{(2)}\right|}\right)\\ &- \mathbf{B}\left(\boldsymbol{K}, \boldsymbol{K}_0 \mid \hat{\boldsymbol{n}} = \frac{\boldsymbol{Q} - \boldsymbol{\xi}^{(1)} - \boldsymbol{\xi}^{(2)}}{\left|\boldsymbol{Q} - \boldsymbol{\xi}^{(1)} - \boldsymbol{\xi}^{(2)}\right|}\right)\Bigg\} + \mathbf{T}_1\left(\boldsymbol{K}, \boldsymbol{K}_0; \boldsymbol{\xi}^{(1)} + \boldsymbol{\xi}^{(2)}\right)\\ &- \mathbf{T}_1\left(\boldsymbol{K}, \boldsymbol{K}_0; \boldsymbol{\xi}^{(1)}\right) - \mathbf{T}_1\left(\boldsymbol{K}, \boldsymbol{K}_0; \boldsymbol{\xi}^{(2)}\right).\end{aligned} \tag{101}$$

Note the arguments $\boldsymbol{\xi}^{(1)}$ and $\boldsymbol{\xi}^{(2)}$ appear in an interchange symmetric fashion as required in (38). Note also from equation (86) that

$$Q_{n1} \sec\alpha = \hat{\boldsymbol{n}}' \cdot \left(\boldsymbol{Q} - \boldsymbol{\xi}^{(1)} - \boldsymbol{\xi}^{(2)}\right) \tag{102}$$

when $\boldsymbol{\xi}^{(1)}$ and $\boldsymbol{\xi}^{(2)}$ are taken as the arguments of $\mathbf{T}_2$ in equation (95).

The identities provided can be used to verify that this kernel vanishes when either of the $\boldsymbol{\xi}$ arguments is set to zero, and also that the derivative about the origin in either of the $\boldsymbol{\xi}$ arguments vanishes. Furthermore, it can be shown that the mixed second derivative in $\boldsymbol{\xi}^{(1)}\boldsymbol{\xi}^{(2)}$ vanishes as well. This kernel enables consistency with the SPM2 theory to be reached regardless of the tilt angle α.

5.4 *Shadowing issues*

Although the basic tilt operator $\hat{\boldsymbol{n}} = \hat{\boldsymbol{Q}}$ is defined so that the incidence and scattering directions achieve specular reflection in the tilted frame, the $\mathbf{T}_1$ tilt operator $\hat{\boldsymbol{n}}^{LCA1} = \frac{\boldsymbol{Q}-\boldsymbol{\xi}}{|\boldsymbol{Q}-\boldsymbol{\xi}|}$ includes a perturbation from this geometry. This tilt angle can become arbitrarily large as the argument $\boldsymbol{\xi}$ becomes large, leading to the possibility of shadowing in the tilted geometry used to evaluate $\mathbf{B}$. Here shadowing is separated into 'incidence' and 'scatter' shadowing, defined respectively, through

$$-\hat{\boldsymbol{n}}^{LCA1} \cdot \boldsymbol{K}_0 < 0 \tag{103}$$

$$\hat{\boldsymbol{n}}^{LCA1} \cdot \boldsymbol{K} < 0. \tag{104}$$

Given the definition of $\hat{\boldsymbol{n}}^{LCA1}$, it is possible to express these conditions in terms of limits on the argument $\boldsymbol{\xi}$.

To simplify this discussion in terms of purely geometrical effects, we adopt a coordinate system in which the vertical direction is labeled $\hat{\boldsymbol{z}}$, and the horizontal directions $\hat{\boldsymbol{x}}$ and $\hat{\boldsymbol{y}}$. Define incidence and scattering propagation angles (θ_i, θ_s) through use of the vertical components of the propagation vectors:

$$q_0 = -\hat{\boldsymbol{z}} \cdot \boldsymbol{K}_0 = K \cos\theta_i \tag{105}$$

$$q_k = \hat{\boldsymbol{z}} \cdot \boldsymbol{K} = K \cos\theta_s. \tag{106}$$

In addition, we specify the horizontal coordinates through

$$\boldsymbol{k}_0 = \hat{x} K \sin\theta_i \tag{107}$$

$$\boldsymbol{k} = K \sin\theta_s (\hat{x} \cos\phi_s + \hat{y} \sin\phi_s). \tag{108}$$

There is no loss of generality in these definitions, as azimuthal rotations of the incidence direction can be accomplished by rotating the surface properties.

Shadowing of the incident wave in the tilted frame now occurs whenever

$$\xi_x < \xi_{x1} = -\frac{K}{\sin\theta_i} F(\theta_i, \theta_s, \phi_s) \tag{109}$$

where

$$F(\theta_i, \theta_s, \phi_s) = 1 + \cos\theta_i \cos\theta_s - \sin\theta_i \sin\theta_s \cos\phi_s. \tag{110}$$

This is a vertical line in the (ξ_x, ξ_y) plane, parallel to the ξ_y axis, and in the second and third quadrants. Similarly, shadowing of the scattered wave in the tilted frame occurs for

$$\xi_x \cos\phi_s + \xi_y \sin\phi_s > \frac{K}{\sin\theta_s} F(\theta_i, \theta_s, \phi_s). \tag{111}$$

This is a line of slope $-\cot\phi_s$ in the (ξ_x, ξ_y) plane; the ξ_x intercept of this line is denoted as ξ_{x2}.

Figure 1 is a plot illustrating these boundaries in the (ξ_x, ξ_y) plane, for $\theta_i = 30^\circ$, $\theta_s = 50^\circ$, and $\phi_s = 45^\circ$; only between the two lines of the figure is no shadowing obtained. Note that the above discussion has focused on shadowing issues involved in computing $\mathbf{T}_1$, but the analysis is very similar for shadowing in $\mathbf{T}_2$ given that the tilt in this case is related in a similar fashion to $\boldsymbol{\xi_1} + \boldsymbol{\xi_2}$.

When shadowing occurs, it is not possible to compute the tilted $\mathbf{B}$ or $\mathbf{B}_2$ quantities needed in the LCA kernels. However, the Kirchhoff quantities in $\mathbf{T}_1$ and $\mathbf{T}_2$ are not affected as there is no tilting involved in their evaluation. Because the tilted $\mathbf{B}$ and $\mathbf{B}_2$ functions approach zero as the incidence and/or scatter propagation directions become shadowed, it is reasonable to define $\mathbf{T}_1$ and $\mathbf{T}_2$ in such shadowed regions by simply setting the shadowed $\mathbf{B}$ or $\mathbf{B}_2$ quantities to zero. This procedure ensures that no discontinuities are introduced into the LCA kernels when shadowing is encountered.

6. Sample results

6.1 *LCA2 for 3D penetrable 'Gaussian' surfaces*

Results are first illustrated to compare the existing and new LCA2 theories for incoherent bistatic scattering from a 3D penetrable surface. The surface is modeled as a Gaussian

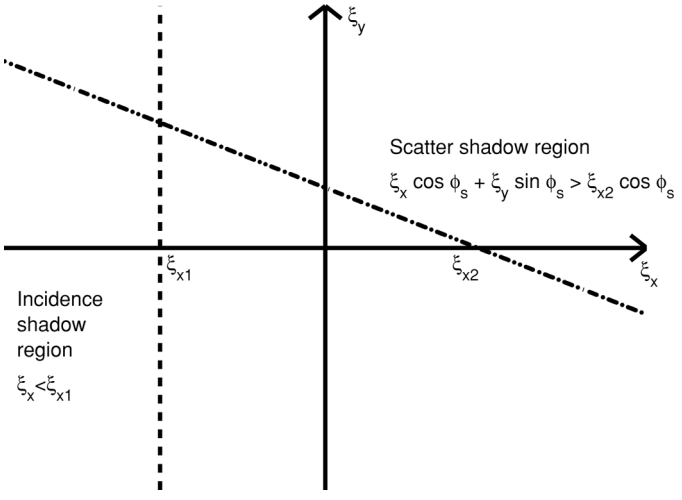

Figure 1. Shadowed regions in the ξ_x,ξ_y domain.

stochastic process with an isotropic Gaussian correlation function, so that surface statistics are completely specified by the rms height (σ) and correlation length (l) parameters. The coordinate system utilized in describing the scattering amplitude is such that the mean value of the surface profile (i.e. along the vertical axis) is zero; this is an 'untilted' coordinate system. Equations for ensemble averaged normalized radar cross sections (NRCS) in this case have been presented in [21] for the SSA theory; LCA ensemble averaged results have an identical form under replacement of the appropriate kernel functions. Using the LCA2 model, the resulting NRCS consists of three terms, involving powers in the two LCA field series terms and the correlation between these two terms. The first NRCS is identical to the KA1 NRCS, with the additional two terms providing corrections. Note that the third series term (involving $\mathbf{T}_1^2$) is a fourth order correction, and is the same order as the correlation between the first field series term and the $\mathbf{T}_2$ term. However, the $\mathbf{T}_2$ contribution is omitted here due to the computational complexity of implementing the $\mathbf{T}_2$ formulation for 3D scattering problems. This will be considered in future work.

Expressions from [21] require both spatial and Fourier (i.e. $\boldsymbol{\xi}$) 2D integrations, which were performed numerically for the cases of interest. Note these integrations can be de-coupled through use of an FFT algorithm, so that a full quadruple integration is not required. The overall LCA2 computation scales with the number of points discretizing the surface (N) as N due to this decoupling of integrations. A CPU time of approximately 2 s per RCS computation on an 800 MHz Pentium processor was required to obtain all three LCA2 cross section terms using a surface discretization of 256 by 256 points ($N = 65536$).

Results of the existing and new LCA2 theories are compared with those from the two-series term SSA and from a Monte Carlo simulation using the method of moments (MOM). The latter utilized 50 realizations, and results were computed using the canonical grid technique [22] in a four scalar function unknown method of moments for a penetrable surface [23] to improve computational efficiency. MOM surfaces sizes were $16\lambda \times 16\lambda$ sampled in 128×128 points, and the 'tapered' incident field described in [22] with $g = 5$ was used to eliminate edge scattering effects. To make the results shown comparable to those in the literature, the local polarization basis (equation (25)) is utilized in describing the results presented. Note use of the tapered incident field causes inaccuracies for large bistatic scattering angles and for cross-polarized predictions, so method of moments results are only included for co-polarized

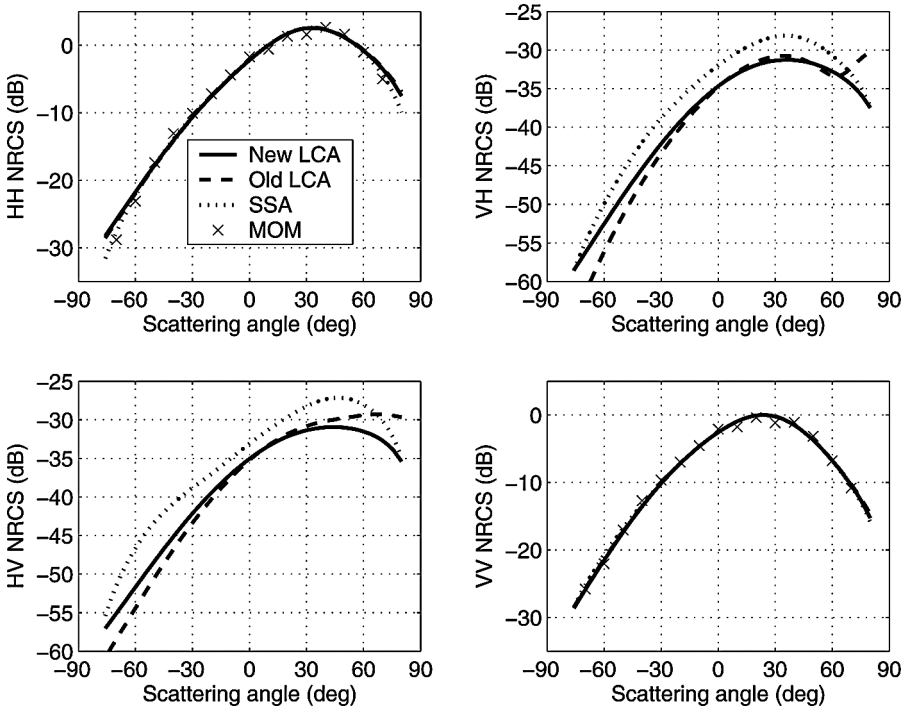

Figure 2. Normalized radar cross-sections for a Gaussian rough surface, $K\sigma = 1$, $Kl = 6$, $\epsilon = 4 + i$, $\theta_i = 30^\circ$.

predictions at scattering angles within 70°. Computational times for this numerical approach were dramatically larger (on the order of tens of CPU hours) compared to those required for LCA2.

Figure 2 illustrates in-plane bistatic NRCS predictions for $K\sigma = 1$, $Kl = 6$, and surface relative permittivity $\epsilon = 4 + i$. The incident field impinges upon the surface at $\theta_i = 30^\circ$, and the polar scattering angle used in the figure is defined so that $\theta_s = 30^\circ$ is specular scattering while $\theta_s = -30^\circ$ is backscattering. Results in all four NRCS polarizations are plotted: the second index of the $\alpha\beta$ notation (*HV*, for example) indicates the incident polarization. Co-polarized (*HH* and *VV*) results show little difference between the SSA2, existing LCA2, and new LCA2 theories, and all are in good agreement with the MOM simulation. Some evidence of a slight over-prediction of HH cross-sections by both the old and new LCA2 theories is present at large bistatic scattering angles. A larger difference among theories is observed in cross polarized predictions; here the new LCA model avoids some of the apparent non-physical behaviors of the existing LCA at large scattering angles. It should be expected that the new LCA model should provide an improved cross-polarized prediction due to the importance of out-of-plane tilting in obtaining cross-polarized fields; the existing LCA model limitation to first order in surface tilt likely introduces the unusual behaviors observed. Note all cross-polarized predictions are obtained from the second field series term, as the KA1 prediction for cross-polarized NRCS vanishes in the plane of incidence. SSA2 cross-polarized results are generally larger than those of either LCA theory, as might be expected due to the importance of $\mathbf{B}_2$ in this polarization. It should be expected that inclusion of the third LCA series term would likely yield a closer match between SSA and LCA theories for cross-pol results.

To highlight the differences between the existing and new LCA predictions for co-polarized cross sections, figure 3 plots the correction to the dominant KA1 term arising from the second

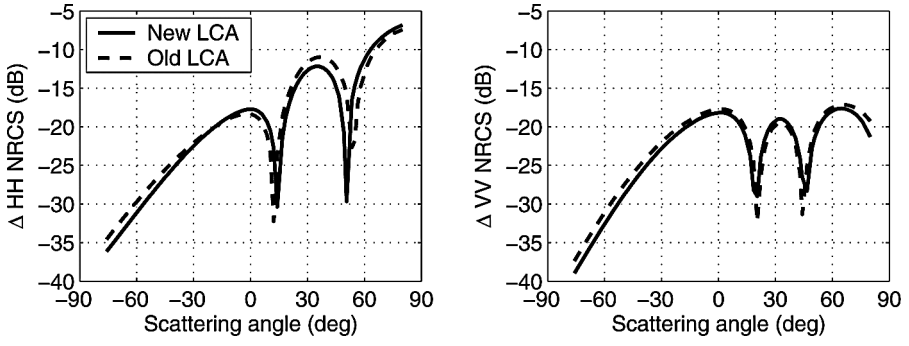

Figure 3. LCA2 corrections to KA1 predictions for a Gaussian rough surface, $K\sigma = 1, Kl = 6, \epsilon = 4+i, \theta_i = 30^\circ$.

and third cross-section corrections. Predictions of the existing and new LCA theories again seem similar, although larger differences are observed (although still insignificant compared to KA1) than in figure 2. The 'nulls' in these plots are due to a sign change in the corrections, with the HH results beginning as negative values (i.e. decreasing the KA1 prediction) at negative scattering angles, then becoming positive, then negative again. The VV results have an opposite trend in their signs versus the scattering angle.

Figures 4 and 5 are analogous to figures 1 and 2, but for the case $K\sigma = 0.5$ and $Kl = 3$ (i.e. the frequency has been decreased by a factor of two.) Results in terms of relationships among theories are generally similar, although here the existing LCA cross-polarized prediction seems even less reliable. Note the small MOM predictions obtained near specular angles are due to

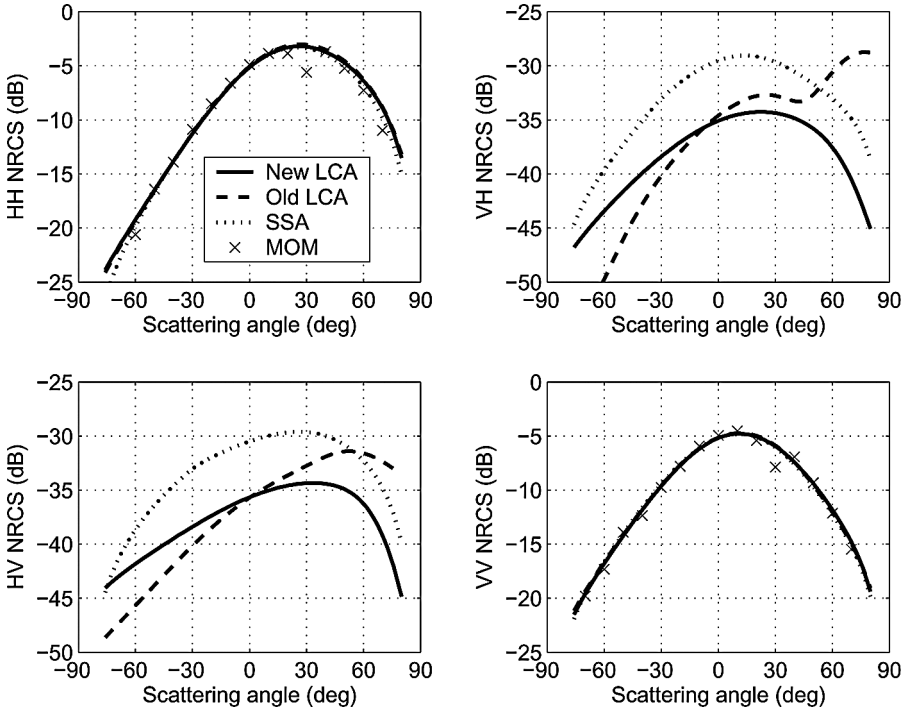

Figure 4. Normalized radar cross-sections for a Gaussian rough surface, $K\sigma = 0.5$, $Kl = 3$, $\epsilon = 4 + i$, $\theta_i = 30^\circ$.

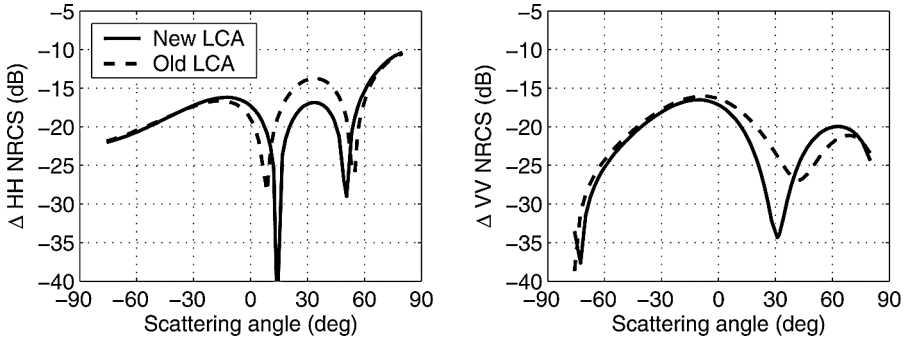

Figure 5. LCA2 corrections to KA1 predictions for a Gaussian rough surface, $K\sigma = 0.5$, $Kl = 3$, $\epsilon = 4 + i$, $\theta_i = 30^\circ$.

difficulties in removing the coherent scattered field in the numerical simulation, and should not be taken as accurate.

6.2 *LCA3 for 2D Dirichlet sinusoidal gratings*

Although implementation of the third LCA series term for 3D scattering problems has not been completed at this time, a study using Dirichlet sinusoidal gratings was performed in order to confirm convergence of the LCA theory to the SPM2 limit. The surfaces considered are of the form

$$h(x) = a \sin\left(\frac{2\pi}{P}x\right), \tag{112}$$

where a is the amplitude of the grating and P is its period, both reported in units of electromagnetic wavelengths. Results are presented in terms of bistatically scattered Floquet mode amplitudes in the plane of the grating; these Floquet modes satisfy the grating relation

$$\boldsymbol{k} = \boldsymbol{k}_0 + \frac{2\pi n}{P} \tag{113}$$

where n is the mode number. Mode amplitudes are normalized such that the sum of the amplitude squared of all mode amplitudes is unity. This geometry is of interest due to its previous utilization in several studies [20, 24].

Studies comparing the existing and new LCA2 theory were performed, and again showed only minor differences in scattered mode amplitude and phase results. However the inclusion of LCA3 now allows verification that the LCA3 theory reproduces SPM2 predictions in the small surface height limit. Figure 6 plots the percent error in KA1, existing LCA2, new LCA2, and LCA3 predictions of scattered Floquet mode complex amplitudes, for $a = 0.01\lambda$, $P = 5\lambda$, and $\theta_i = 61.35^\circ$. Percent errors were defined in terms of the difference between the predicted complex mode amplitudes and those obtained from a 20th-order numerical SPM solution [3], relative to the 20th-order SPM solution. Errors for the specular mode (mode 0) were determined in terms of corrections to the flat surface value of -1. Results show inclusion of the LCA3 prediction to yield dramatic reductions in obtained errors, particularly for the zero mode, where it is known that the SPM1 correction vanishes. Note the numerical results show a slight increase in error when using LCA3 for the -1 mode, although the differences are sufficiently small to make these predictions particularly sensitive to errors in the computation. In addition the error in prediction of the -3 mode is larger than other modes; this is due to the

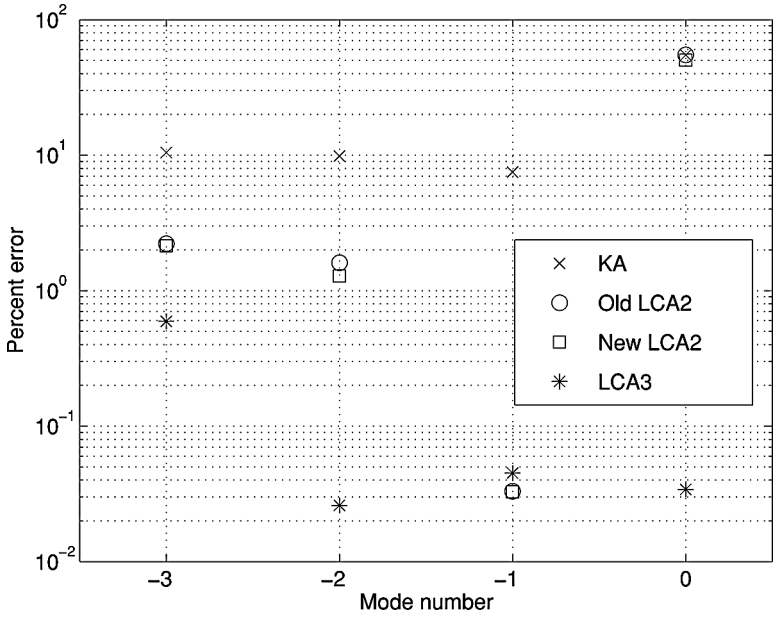

Figure 6. Percent error in mode scattered fields for $a = 0.01\lambda$, $P = 5\lambda$, $\sin\theta_i = 61.35^\circ$.

fact that the SPM2 solution for a sinusoidal grating predicts zero amplitude for the -3 mode, so that SPM3 kernels can be important for this extremely small amplitude mode. Even without the use of any SPM3 kernels, the LCA3 solution obtains an error of less than one percent in predicting the mode amplitude. Overall these results serve to verify the reduction of LCA3 to SPM2 in the low frequency limit.

7. Conclusion

The local curvature approximation (LCA) has been generalized to achieve conformity with SPM1 for an arbitrary surface tilt, as well as conformity with the second-order SPM theory for arbitrary tilt when a third LCA series term is included. Although the numerical examples illustrated showed only minor differences between the new and existing LCA2 models, it should be expected that inclusion of the LCA3 term in future studies will enhance the ability of the theory in the prediction of cross-polarized cross-sections particularly. Although the LCA3 term is computationally complex (involving a sixfold integration for scattered fields in 3D problems), other terms of similar complexity have been included in previous studies. Recent efforts by the authors have focused on a 'reduced' LCA3 model, in which a fourfold integration is used to approximate the full three-term series; this work will be reported in future publications. Several new identities involving the KA and SPM kernels have been obtained as byproducts in the derivation; these identities may find application in future theoretical studies of rough surface scattering. Routines for computing the new LCA3 kernels are available upon request to the authors.

Appendix A. First-order SPM kernels for electromagnetic scattering from a penetrable interface

Consider vector electromagnetic scattering from an interface between free space and a medium with relative permittivity ϵ. The first order SPM kernels B_{hh}, B_{vh}, B_{hv}, and B_{vv} are given by

$-i\hat{\boldsymbol{n}}\cdot\boldsymbol{K}$ multiplied by equations (75), (76), (79), and (80) of [18], respectively. Although [18] uses a different notation than the current formulation, the transformation of $\hat{\boldsymbol{n}}\cdot\boldsymbol{K}_0$ to k_{zi}, $\hat{\boldsymbol{n}}\cdot\boldsymbol{K}$ to $k_{zn'm'}$, and $\boldsymbol{\xi}$ to $\boldsymbol{k}_{nm}$ makes the kernel definitions clear. Specifically, this process results in

$$B_{hh}(\boldsymbol{K},\boldsymbol{K}_0\mid\hat{\boldsymbol{n}}) = \frac{2q_kq_0(\epsilon-1)K^2\hat{\boldsymbol{k}}\cdot\hat{\boldsymbol{k}}_0}{(q_k+q_k')(q_0+q_0')} \tag{A.1}$$

$$B_{vh}(\boldsymbol{K},\boldsymbol{K}_0\mid\hat{\boldsymbol{n}}) = \frac{2q_kq_0(\epsilon-1)K^2}{(\epsilon q_k+q_k')(q_0+q_0')}\frac{q_k'}{K}(\hat{\boldsymbol{n}}\cdot(\hat{\boldsymbol{k}}_0\times\hat{\boldsymbol{k}})) \tag{A.2}$$

$$B_{hv}(\boldsymbol{K},\boldsymbol{K}_0\mid\hat{\boldsymbol{n}}) = \frac{2q_kq_0(\epsilon-1)K^2}{(q_k+q_k')(\epsilon q_0+q_0')}\frac{q_0'}{K}(\hat{\boldsymbol{n}}\cdot(\hat{\boldsymbol{k}}_0\times\hat{\boldsymbol{k}})) \tag{A.3}$$

$$B_{vv}(\boldsymbol{K},\boldsymbol{K}_0\mid\hat{\boldsymbol{n}}) = \frac{2q_kq_0(\epsilon-1)K^2}{(\epsilon q_k+q_k')(\epsilon q_0+q_0')}\frac{(\epsilon|\boldsymbol{k}||\boldsymbol{k}_0|-q_k'q_0'\hat{\boldsymbol{k}}\cdot\hat{\boldsymbol{k}}_0)}{K^2} \tag{A.4}$$

where

$$q_k = \hat{\boldsymbol{n}}\cdot\boldsymbol{K} \tag{A.5}$$

$$q_0 = -\hat{\boldsymbol{n}}\cdot\boldsymbol{K}_0 \tag{A.6}$$

$$\boldsymbol{k} = \mathbf{P}_{\parallel}(\hat{\boldsymbol{n}})\cdot\boldsymbol{K} \tag{A.7}$$

$$\boldsymbol{k}_0 = \mathbf{P}_{\parallel}(\hat{\boldsymbol{n}})\cdot\boldsymbol{K}_0 \tag{A.8}$$

$$q_k' = \sqrt{\epsilon K^2-\boldsymbol{k}\cdot\boldsymbol{k}} \tag{A.9}$$

$$q_0' = \sqrt{\epsilon K^2-\boldsymbol{k}_0\cdot\boldsymbol{k}_0}. \tag{A.10}$$

These quantities are in the local polarization basis (equations (25)) and are to be transformed with equations (27)–(30) before their further use.

Appendix B. Second-order SPM kernels for electromagnetic scattering from a penetrable interface

Consider vector electromagnetic scattering from an interface between free space and a medium with relative permittivity ϵ. At second order, the coefficients $B_{2,hh}$, $B_{2,vh}$, $B_{2,hv}$, and $B_{2,vv}$ are given by $(\hat{\boldsymbol{n}}\cdot\boldsymbol{K})\,/\,(\hat{\boldsymbol{n}}\cdot\boldsymbol{Q})$ multiplied by equations (88), (89), (95), and (96) of [18], respectively. Specifically,

$$B_{2,hh}(\boldsymbol{K},\boldsymbol{K}_0;\boldsymbol{\xi}\mid\hat{\boldsymbol{n}}) = \frac{2q_kq_0(\epsilon-1)K^2}{Q_n(q_k+q_k')(q_0+q_0')}\Bigg\{C_1C_2(R_1+q_k')+S_1S_2(q_k'+R_2) + \frac{C_3}{2}(q_0'-q_k')\Bigg\} \tag{B.1}$$

$$B_{2,vh}(\boldsymbol{K},\boldsymbol{K}_0;\boldsymbol{\xi}\mid\hat{\boldsymbol{n}}) = \frac{2q_kq_0(\epsilon-1)K^2}{Q_n(\epsilon q_k+q_k')(q_0+q_0')}\Bigg\{S_1C_2\left(\epsilon K+\frac{q_k'}{K}R_1\right)-C_1S_2\left(\epsilon K+\frac{q_k'}{K}R_2\right) + S_2\frac{\epsilon|\boldsymbol{k}|}{K}R_3+\frac{S_3}{2}\left(\epsilon K-\frac{q_k'}{K}q_0'\right)\Bigg\} \tag{B.2}$$

$$B_{2,hv}(\boldsymbol{K},\boldsymbol{K}_0;\boldsymbol{\xi}|\hat{\boldsymbol{n}}) = \frac{2q_kq_0(\epsilon-1)K^2}{Q_n(q_k+q_k')(\epsilon q_0+q_0')}\Bigg\{ -C_1S_2\left(\frac{q_0'}{K}\right)(R_1+q_k') + S_1C_2\left(\frac{q_0'}{K}\right)(q_k'+R_2) - S_1\left(\frac{\epsilon|\boldsymbol{k}_0|}{K}\right)R_3 - \frac{S_3}{2}\left(\epsilon K - \frac{q_k'}{K}q_0'\right)\Bigg\} \quad \text{(B.3)}$$

$$B_{2,vv}(\boldsymbol{K},\boldsymbol{K}_0;\boldsymbol{\xi}|\hat{\boldsymbol{n}}) = \frac{2q_kq_0(\epsilon-1)K^2}{Q_n(\epsilon q_k+q_k')(\epsilon q_0+q_0')}\Bigg\{ -S_1S_2\left(\frac{q_0'}{K}\right)\left(\epsilon K+\frac{q_k'}{K}R_1\right) - C_1C_2\left(\frac{q_0'}{K}\right)\left(\epsilon K+\frac{q_k'}{K}R_2\right) + C_1\left(\frac{\epsilon|\boldsymbol{k}_0|q_k'}{K^2}\right)R_3 + \left(\frac{\epsilon|\boldsymbol{k}|R_3}{K^2}\right)\left(q_0'C_2+\frac{|\boldsymbol{\chi}||\boldsymbol{k}_0|}{K^2}R_1\right) + \frac{C_3}{2}(\epsilon q_0'-\epsilon q_k')\Bigg\} \quad \text{(B.4)}$$

where

$$\boldsymbol{\chi} = \mathbf{P}_{\|}(\hat{\boldsymbol{n}})\cdot\boldsymbol{\xi} \quad \text{(B.5)}$$

$$q_\chi = \sqrt{K^2-\boldsymbol{\chi}\cdot\boldsymbol{\chi}} \quad \text{(B.6)}$$

$$q_\chi' = \sqrt{\epsilon K^2-\boldsymbol{\chi}\cdot\boldsymbol{\chi}} \quad \text{(B.7)}$$

$$R_1 = q_\chi - q_\chi' \quad \text{(B.8)}$$

$$R_2 = \frac{q_\chi q_\chi'(1-\epsilon)}{\epsilon q_\chi + q_\chi'} \quad \text{(B.9)}$$

$$R_3 = \frac{|\boldsymbol{\chi}|K^2}{|\boldsymbol{\chi}|^2+q_\chi q_\chi'} \quad \text{(B.10)}$$

$$C_1 = \hat{\boldsymbol{\chi}}\cdot\hat{\boldsymbol{k}} \quad \text{(B.11)}$$

$$C_2 = \hat{\boldsymbol{\chi}}\cdot\hat{\boldsymbol{k}}_0 \quad \text{(B.12)}$$

$$C_3 = \hat{\boldsymbol{k}}\cdot\hat{\boldsymbol{k}}_0 \quad \text{(B.13)}$$

$$S_1 = \hat{\boldsymbol{n}}\cdot(\hat{\boldsymbol{\chi}}\times\hat{\boldsymbol{k}}) \quad \text{(B.14)}$$

$$S_2 = \hat{\boldsymbol{n}}\cdot(\hat{\boldsymbol{\chi}}\times\hat{\boldsymbol{k}}_0) \quad \text{(B.15)}$$

$$S_3 = \hat{\boldsymbol{n}}\cdot(\hat{\boldsymbol{k}}\times\hat{\boldsymbol{k}}_0) \quad \text{(B.16)}$$

and $\boldsymbol{\xi}$ is an arbitrary three-dimensional vector. The definitions of equations (A.5)–(A.10) are also used above. These quantities must be transformed into the global polarization basis with equations (27)–(30) before their further use.

It is here noted that the $\mathbf{B_2}$ quantities are not uniquely defined, as it is possible to add to these quantities functions that vanish in the integration of equation (24). However, the LCA3 form used removes this non-uniqueness, so that the non-uniqueness of $\mathbf{B_2}$ is irrelevant.

References

[1] Rice, S. O., 1951, Reflection of electromagnetic waves from slightly rough surfaces. *Communications in Pure and Applied Mathematics*, **4**, 351–378.

[2] Valenzuela, G. R., 1967, Depolarization of EM waves by slightly rough surfaces. *IEEE Transactions on Antennas and Propagation*, **15**(4), 552–557.

[3] Demir, M. A., and Johnson, J. T., 2003, Fourth- and higher-order small-perturbation solution for scattering from dielectric rough surfaces. *Journal of the Optical Society of America*, **20**(12), 2330–2337.

[4] Beckmann, P. and Spizzichino, A., 1963, *The Scattering of Electromagnetic Waves from Rough Surfaces*. (Oxford: Pergamon Press).

[5] Jin, Y.-Q., and Lax, M., 1990, Backscattering enhancement from a randomly rough surface. *Physics Reviews B*, **42**(16), 9819–9829.

[6] Elfouhaily, T. and Guérin, C. A., 2004, A critical survey of approximate scattering wave theories from random rough surfaces. *Waves in Random Media*, **14**, R1–R40.

[7] Elfouhaily, T., Guignard, S., Awadallah, R., and Thompson, D. R., 2003, Local and non-local curvature approximation: A new asymptotic theory for wave scattering. *Waves in Random Media*, **13**(4), 321–338.

[8] Elfouhaily, T., Guignard, S., and Thompson, D. R., 2003, Formal tilt invariance of the local curvature approximation. *Waves in Random Media*, **13**(4), L7–L11.

[9] Elfouhaily, T., Joelson, M., Guignard, S., and Thompson, D. R., 2003, Analytical comparison between the surface current integral equation and the second-order small-slope approximation. *Waves in Random Media*, **13**(3), 165–176.

[10] Rodriguez, E., 1989, Beyond the Kirchhoff approximation. *Radio Science*, **24**(5), 681–693.

[11] Rodriguez, E., 1991, Beyond the Kirchhoff approximation II. Electromagnetic scattering. *Radio Science*, **26**(1), 121–132.

[12] Rodriguez, E., and Kim, Y., 1992, A unified perturbation expansion for surface scattering. *Radio Science*, **27**, 79–93.

[13] Charnotskii, M. I., and Tatarskii, V. I., 1995, Tilt-invariant theory of rough-surface scattering. I. *Waves in Random Media*, **5**(4), 361–380.

[14] Voronovich, A. G., 1985, Small-slope approximation in wave scattering from rough surfaces. *Soviet Physics JETP*, **62**(1), 65–70.

[15] Voronovich, A. G., 1994, Small-slope approximation for electromagnetic wave scattering at a rough interface of two dielectric half-spaces. *Waves in Random Media*, 4(3), 337–367.

[16] Voronovich, A. G., 1994, *Wave Scattering from Rough Surfaces*, ser. Springer Series on Wave Phenomena. Springer.

[17] Voronovich, A. G., 2002, The effect of the modulation of Bragg scattering in small-slope approximation. *Waves in Random Media*, **12**(3), 341–349.

[18] Johnson, J. T., 1999, Third order small perturbation method for scattering from dielectric rough surfaces. *Journal of the Optical Society America*, **16**, 2720–2726.

[19] Tsang, L., Kong, J. A., and Shin, R., 1985, *Theory of Microwave Remote Sensing* (New York: Wiley-Interscience).

[20] Voronovich, A. G., 1996, Non-local small-slope approximation for wave scattering from rough surfaces. *Waves in Random Media*, **6**(2), 151–167.

[21] Gilbert, M. S., and Johnson, J. T., 2003, A study of the higher-order small-slope approximation for scattering from a gaussian surface. *Waves in Random Media*, **13**, 137–143.

[22] Pak, K., Tsang, L., and Johnson, J. T., 1997, Numerical simulations and backscattering enhancement of electromagnetic waves from two-dimensional dielectric random rough surfaces with the sparse canonical grid method. *Journal of the Optical Society of America*, **14**(7), 1515–1529.

[23] Johnson, J. T., Shin, R. T., Kong, J. A., Tsang, L., and Pak, K., 1999, A numerical study of ocean polarimetric thermal emission. *IEEE Transactions in Geoscience and Remote Sensing*, **37**(1), 8–20.

[24] Elfouhaily, T. M., Bourlier, C., and Johnson, J. T., 2004, Two families of non-local scattering models and the weighted curvature approximation. *Waves in Random Media*, **14**, 1–18.

Query

Q1. Au: Pls. provide keywords and PACS nos. deleted here ok?